mathematics

Article

Developed Gorilla Troops Technique for Optimal Power Flow Problem in Electrical Power Systems

Abdullah Shaheen [1], Ahmed Ginidi [1], Ragab El-Sehiemy [2,*], Abdallah Elsayed [3], Ehab Elattar [4] and Hassen T. Dorrah [5]

1 Department of Electrical Engineering, Faculty of Engineering, Suez University, Suez 43533, Egypt; abdullahshaheen2015@gmail.com (A.S.); ahmed.ginidi@eng.suezuni.edu.eg (A.G.)
2 Department of Electrical Engineering, Faculty of Engineering, Kafrelsheikh University, Kafrelsheikh 33516, Egypt
3 Department of Electrical Engineering, Faculty of Engineering, Damietta University, Damietta 34517, Egypt; am.elsherif@yahoo.com
4 Department of Electrical Engineering, College of Engineering, Taif University, Taif 21944, Saudi Arabia; e.elattar@tu.edu.sa
5 Department of Electrical Engineering, Cairo University, Giza 12613, Egypt; dorrahht@aol.com
* Correspondence: elsehiemy@eng.kfs.edu.eg

Abstract: This paper presents a developed solution based on gorilla troops optimization technique for OPFP in EPSs. The GTOT is motivated by gorillas' group behaviors in which several methods are replicated, such as migration to an unfamiliar location, traveling to other gorillas, migration toward a specific spot, accompanying the silverback, and competing for adult females. The multi-dimension OPFP in EPSs is examined in this article with numerous optimizing objectives of fuel cost, power losses, and harmful pollutants. The system's power demand and transmission losses must be met as well. The developed GTOT's evaluation is conducted using an IEEE standard 30-bus EPS and practical EPS from Egypt. The created GTOT is employed in numerous evaluations and statistical analyses using many modern methods such as CST, GWT, ISHT, NBT, and SST. When compared to other similar approaches in the literature, the simulated results demonstrate the GTOT's solution efficiency and robustness.

Keywords: gorilla troops optimization technique; electrical power systems; optimal power flow; harmful pollutants; fuel costs; power losses

MSC: 90-08

Citation: Shaheen, A.; Ginidi, A.; El-Sehiemy, R.; Elsayed, A.; Elattar, E.; Dorrah, H.T. Developed Gorilla Troops Technique for Optimal Power Flow Problem in Electrical Power Systems. *Mathematics* **2022**, *10*, 1636. https://doi.org/10.3390/math10101636

Received: 2 April 2022
Accepted: 9 May 2022
Published: 11 May 2022

1. Introduction

The optimum operational analysis is critical in determining the projected financial return for electrical networks. The energy supply is shifting around the globe towards sustainability, low carbon content, and high efficiency [1]. The increased load demand acts as an urgent challenge for power system operators. The economic and environmental prospects of power generations in modern power systems are considered the weighty research targets and the key concern of electric utility operators. The OPFP is a non-linear, multi-model issue in EPSs for power system control and operation. Using OPFP, pecuniary and safe operating circumstances of EPSs can be elaborated [2]. The solution of OPFP is currently the principal strategy for controlling and operating the modern power grids [3]. The OPFP can optimize one or even more targets such as cost of fuel, EPS sources pollution, and system losses. These goals may be met while maintaining load flow balancing and keeping operating variables inside the corresponding limitations, including voltages restrictions, transmission network limits, valve constraints, and generator output limits [4].

Various standard mathematic methodologies were proposed to address the OPFP, such as semidefinite programming [5], non-linear programming [6], linear programming [7,8], quadratic programming [9,10], fuzzy linear programming [11], sequential unconstrained minimization technique [12], Newton-based method [13,14] and interior point approach [15–17]. A myriad of these approaches can effectively impose inequality restrictions and possess high convergence properties. Nevertheless, these conventional methods cannot generate the real optimal results because they rely on the initial settings, and consequently, they may get stuck in a local minimum. Additionally, every approach should be modeled with particular variants for OPFP, and they cannot deal with variables of discrete and integer natures smoothly. Hence, it is pivotal to develop metaheuristic techniques to overcome the mentioned disadvantages. The rapid growth of computers in the last two decades has led to a trend to solve diverse OPFP challenges using several heuristic (population-based) techniques [18,19]. Examples of these population-based heuristics are CBOA [20], BBO [21], PSO [22,23], HGWODE [24], GA [25], EMM [26], TLBO [27], and SAO [28].

In addition to that, recent techniques have been manifested to attain the solution of the large-scale OPFP: QMFT [29], COA [30], CSSO [31], and WCEMFT [32]. Moreover, a multi-group strategy was combined with the marine predators method to subdivide the original population into numerous separate groups in order to reduce the operation costs of power systems to maximize the economic advantages [33]. To tackle the economic dispatch difficulties of thermal generators, the DE method based on nondominated sorting was used to reduce pollution emissions and economic costs taking into account the dynamical schedule of thermal power units with consideration of ramp-rate, valve-point impact, and balance of power [34]. This method has been applied to two different systems with 13 and 40 thermal generating units.

Various augmentations of the algorithm strategies can be used to identify the best OPFP solution. An emended moth swarm algorithm (EMSA), in [35], has been presented to the OPFP with adjustment of quasi-opposition-based learning. Moreover, AGST, developed in [36], has been illustrated and applied with three objectives which are the fuel cost, emission, and losses taking into consideration different equality and inequality constraints. Additionally, ISSO was presented to minimize fuel costs, emissions, and power losses [37] by adjusting the movement technique of male and female spiders to acceptable ratios. In [38], a modified JAYA has been manifested by proposing modifying the equation for solutions that rely on the worst and best solutions, and technique has been applied to fuel cost, emission, voltage profile, and losses functions. Furthermore, IADE has been handled, in [39], with the self-adaptive penalty constraint technique and applied to the OPFP. To enhance exploration capability and the solution optimality convergence, quasi-oppositional-based learning has emerged with the Jaya technique in [40] to attain the OPFP solution. Moreover, an improved NSGA-III has been utilized with constraint management and decreasing selecting attempts to solve fuel costs, losses, and emission functions, as depicted in [41]. In [42], MRFO was implemented for EPSs to decrease the costs of fuel, losses, and pollution with/without the inclusion of voltage-source-converter stations.

Recently, a technique named gorilla troops optimization technique (GTOT) [43] proposed by (Benyamin Abdollahzadeh et al.) is developed in this article for multi-dimension OPFP in EPSs by adding valve constraint to the OPFP. GTOT is developed with five strategies to enlighten the exploitation and exploration of the optimization progression. To deal with the exploration phase, three strategies are verified: migration to a not recognized place, movement to other gorillas, and migration to a recognized location. Nevertheless, in the exploitation phase, two strategies are verified: follow the silverback and struggle for adult females. The superiority of this technique is that it has few parameters to be adjusted as well as it is simple to be implemented for engineering applications. The evaluation of GTOT quality is illustrated by applying it to various systems: IEEE standard 30 bus and practical WD Area. The results of the GTOT are compared with recent techniques and other existing techniques to demonstrate its efficacy and superiority between these techniques. The following are important contributions discussed in this work.

- The designed GTOT is exploited to reduce different target functions for minimizing the fuel costs, power losses, and pollutant emissions related to EPSs and applied on the IEEE standard 30 bus and practical WD.
- Multi-dimension operations with two or three objectives are developed in this work.
- The developed GTOT outperforms a number of current approaches, including CST, GWT, ISHT, NBT, and SST.
- Statistical analyses and stability assessments are developed in this work to demonstrate the capability of the proposed GTOT in handling the OPFP with different sizes and objective functions.
- The simulation results of related techniques in the literature are compared with the developed GTOT to demonstrate the robustness and solution quality of GTOT.
- Substantial consistency is accompanied by the proposed GTOT for handling the OPFP in EPSs.

The other portions of the whole work are as follows: Section 2 illustrates the GTOT approach. Section 3 establishes the OPFP construction, whereas Section 4 manifests the designed GTOT for OPFP. Furthermore, the simulated findings and discussions are denoted in Section 5, whilst the concluding notes are provided in Section 6.

2. Gorilla Troops Optimization Technique

The gorilla troops optimization technique (GTOT) simulates five strategic options to clarify the optimizing process's exploitation and exploration, as manifested in the following paragraphs.

2.1. Exploration Phase

In GTOT, every gorilla is denoted by a candidate solution, but at every optimizing operational phase, the global optimal solution is designated as a silverback. For the exploratory stage of development, three distinct methods are used. The first one is the movement to an unknown destination to raise GTOT exploration, while the second method is the movement of other gorillas to enhance the consistency between exploratory and exploitation. Moreover, the third method is the gorilla's movement in the path of a recognized destination to raise GTOT capabilities to discover varied computation spaces. In this technique, the factor (Pr) should be supplied in the band [0:1] prior to the optimizing process. When a factor (Pr) is greater than a random number, the movement to an undetermined location strategy is selected [44]. Additionally, if a random number is more than or equal to 50%, a movement in the path of an identifiable place is decided, whereas if a random number is less than 50%, a movement in the path of a recognized site is selected. Those three exploratory tactics can be mathematically stated as follows:

$$GX(g+1) = \begin{cases} LL + rd_1 \times (UL - LL), & \mathrm{Pr} > rand, \\ H \times L + X_r(g) \times (rd_2 - C), & 0.5 \le rand, \\ X(g) + (X(g) - GX_r(t)) \times rd_3 - (X(g) - GX_r(g) \times L^2), & 0.5 > rand \end{cases} \tag{1}$$

$$C = F \times (1 - Iter/MaxIter), \tag{2}$$

$$F = \cos(2 \times rd_4) + 1, \tag{3}$$

$$L = C \times l \tag{4}$$

$$H = Z \times X(g) \tag{5}$$

$$Z = [-C, C]. \tag{6}$$

2.2. Exploitation Phase

In the exploitation stage of GTOT, two methods are used: following the silverback and competing for female adults. Based on factor C and contrasting it to the variable (W) (which can be changed), one of the two methods is selected.

The leader of the gorillas' group is the silverback that can make choices and directs the others to sources of food. If the C is greater than or equal to the value of W, this approach is chosen. Equation (7) can be used to illustrate this phenomenon.

$$GX(g+1) = L \times M(g) \times (X(g) - X_{siverback}) + X(g) \tag{7}$$

$$M(g) = \left(\left| (1/N) \sum_{i=1}^{N} GX_i(g) \right|^{2^L} \right)^{\left(\frac{1}{2^L}\right)} \tag{8}$$

If C is less than W, the next approach is competing for female adults, which is specialized for the evaluation stage. When adolescent gorillas reach adolescence, they engage in a violent rivalry with other males for the selection of female adults. This behavior is formulated as follows:

$$GX(g) = X_{silverback} - (X_{silverback} \times Q - X(g) \times Q) \times A, \tag{9}$$

$$Q = 2 \times rd_5 - 1 \tag{10}$$

$$A = \beta \times E \tag{11}$$

$$E = \begin{cases} N_1 & rand \geq 0.5 \\ N_2 & rand < 0.5 \end{cases} \tag{12}$$

At the end of the exploitation stage, the cost of $GX(g)$ is compared to its counterpart $X(g)$, and if the cost of $GX(g)$ is less than $X(g)$, the $GX(g)$ solution replaces it and becomes the optimal option (silverback). Figure 1 depicts the major processes of the developed GTOT for extracting characteristics from solar cell models [44].

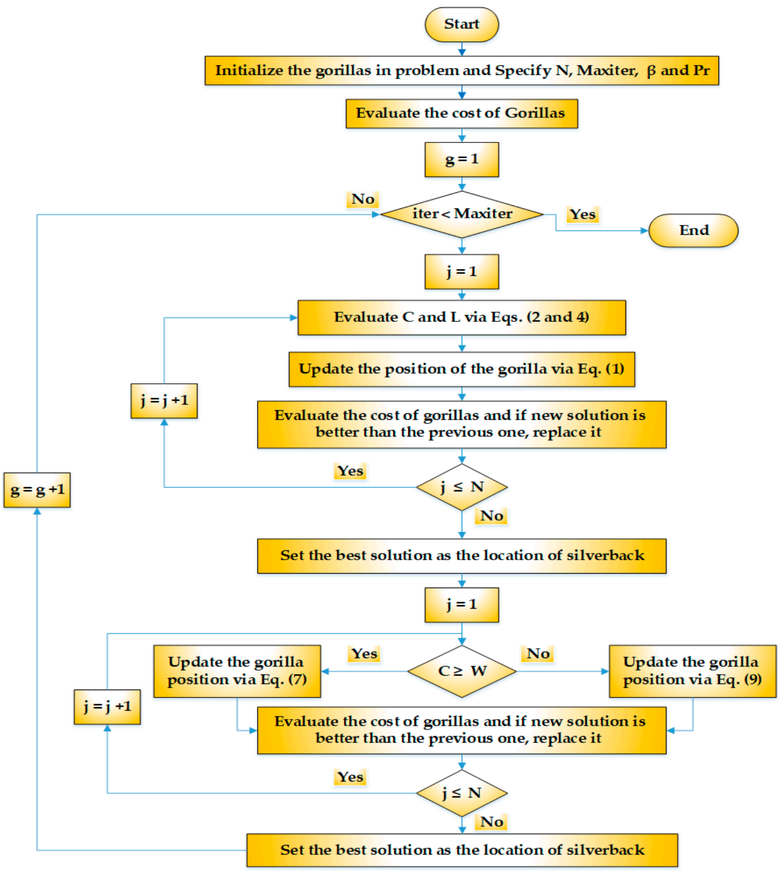

Figure 1. Main steps of the GTOT.

3. Problem Formulation

In OPFP, the dependent and independent variables are represented. To illustrate, the generators' real power output and the reactive power injections of switching capacitors and reactors, voltages of the generators, tap changer settings, the number of on-load tap changers, generators, and reactive power sources, generator reactive power outputs, load bus voltage magnitudes, and transmission flow limits, number of transmission lines and load buses are the main pillars of OPFP. This problem can be expressed as follows:

$$Min\ OJ = \{OJ_1(x,y), OJ_2(x,y) \ldots, OJ_m(x,y)\} \tag{13}$$

$$\text{Subject to}:\ F(x,y) = 0 \tag{14}$$

$$M(x,y) \leq 0 \tag{15}$$

3.1. Objectives

The primary goal is to calculate the OJ_1 in dollars per hour as follows:

$$OJ_1 = \sum_{k=1}^{Ng} C_k \times {Pg_k}^2 + B_k \times Pg_k + A_k \tag{16}$$

Because of the constant change in steam valves in power plants, the valve-point load influence generates fluctuations in the FCs. As a consequence, the FCs formula is produced by integrating sinusoidal rectifications to the quadratic formula, and OJ_2 can be represented as follows:

$$OJ_2 = \sum_{k=1}^{Ng} C_k \times {Pg_k}^2 + B_k \times Pg_k + A_k + \left| E_k \times (\sin(F_k(Pg_k - Pg_k^{\min}))) \right| \tag{17}$$

The second goal is to minimize OJ_3 from the power plants, which can be formulated as:

$$OJ_3 = \sum_{k=1}^{Ng} (\gamma_k \times {Pg_k}^2 + \beta_k \times Pg_k + \alpha_k)/100 + \zeta_k \times e^{\lambda_k \times Pg_k} \tag{18}$$

The third goal is to minimize the overall power loss throughout the transmission system, which is mathematically stated as:

$$OJ_4 = \sum_{m=1}^{Nb} \sum_{n=1}^{Nb} G_{mn} \times ({V_m}^2 + {V_n}^2 - 2(V_m \times V_n \times \cos\theta_{mn})) \tag{19}$$

3.2. System Constraints

The load flow balance equations, Equations (20) and (21), manifest the equality constraints:

$$Pg_j - PL_j - V_j \times \sum_{k=1}^{Nb} V_k \times (G_{jk} \times \cos\theta_{jk} + B_{jk} \times \sin\theta_{jk}) = 0,\ j = 1,\ \ldots,\ Nb \tag{20}$$

$$QL_j - V_j \times \sum_{k=1}^{Nb} V_k \times (G_{jk} \times \sin\theta_{jk} - B_{jk} \times \cos\theta_{jk}) = 0,\ j = 1, 2,\ \ldots,\ Nb \tag{21}$$

Furthermore, the operating variables and the accompanying restrictions are written as follows:

$$Pg_k^{\min} \leq Pg_k \leq Pg_k^{max},\ k = 1,\ 2,\ \ldots,\ Ng \tag{22}$$

$$Vg_k^{\min} \leq Vg_k \leq Vg_k^{max},\ k = 1,\ 2,\ \ldots,\ Ng \tag{23}$$

$$Qg_k^{\min} \leq Qg_k \leq Qg_k^{max},\ k = 1,\ 2,\ \ldots,\ Ng \tag{24}$$

$$Tap_{Tr}^{\min} \le Tap_{Tr} \le Tap_{Tr}^{max},\ Tr = 1,\ 2,\ \ldots,\ Nt \tag{25}$$

$$Qc_{VAR}^{\min} \le Qc_{VAR} \le Qc_{VAR}^{max},\ VAR = 1,\ 2,\ \ldots,\ Nq \tag{26}$$

$$VL_{j}^{\min} \le VL_{j} \le VL_{j}^{max},\ j = 1,\ 2,\ \ldots,\ NPQ \tag{27}$$

$$\left|S_{fl}\right| \le S_{fl}^{max},\ fl = 1,\ 2,\ \ldots,\ Nf \tag{28}$$

4. Developed Solution-Based GTOT for OPFP in EPSs

The equality and inequality constraints are indeed considered while handling the stated OPFP problem. To satisfy the equality conditions that describe power flow balance models, the NRA is applied. It depicts the steady-state operation of electric grids and meets the balance constraints. Consequently, the NRA is used by MATPOWER and represents a key framework for demonstrating three-phase systems [45].

4.1. Improvement of GTOT for Incorporating Operational Limitations of Independent Variables

The operational limitations of independent variables of Equations (22)–(26) may be rewritten as follows:

$$Pg_{k} = \begin{cases} Pg_{k}^{\min} & if\ Pg_{k} \le Pg_{k}^{\min} \\ Pg_{k}^{max} & if\ Pg_{k} \ge Pg_{k}^{max} \end{cases},\ k = 1,\ 2,\ \ldots,\ Ng \tag{29}$$

$$Vg_{k} = \begin{cases} Vg_{k}^{\min} & if\ Vg_{k} \le Vg_{k}^{\min} \\ Vg_{k}^{max} & if\ Vg_{k} \ge Vg_{k}^{max} \end{cases},\ k = 1,\ 2,\ \ldots,\ Ng \tag{30}$$

$$Qg_{k} = \begin{cases} Qg_{k}^{\min} & if\ Qg_{k} \le Qg_{k}^{\min} \\ Qg_{k}^{max} & if\ Qg_{k} \ge Qg_{k}^{max} \end{cases},\ k = 1,\ 2,\ \ldots,\ Ng \tag{31}$$

$$Tap_{Tr} = \begin{cases} Tap_{Tr}^{\min} & if\ Tap_{Tr} \le Tap_{Tr}^{\min} \\ Tap_{Tr}^{max} & if\ Tap_{Tr} \ge Tap_{Tr}^{max} \end{cases},\ Tr = 1,\ 2,\ \ldots,\ Nt \tag{32}$$

$$Qc_{VAR} = \begin{cases} Qc_{VAR}^{\min} & if\ Qc_{VAR} \le Qc_{VAR}^{\min} \\ Qc_{VAR}^{max} & if\ Qc_{VAR} \ge Qc_{VAR}^{max} \end{cases},\ VAR = 1,\ 2,\ \ldots,\ Nq \tag{33}$$

As shown, the variables continue to reach their limitations, and if one of these surpasses ratings, they are regenerated randomly inside the appropriate constraints.

4.2. Improvement of GTOT for Incorporating Operational Limitations of Dependent Variables

Moreover, the target cost objective expands and penalizes the second category's limitations. Therefore, if the gorilla's location exceeds any of the appropriate constraints, it would be discarded in the next round. Such concepts may be used to construct the contemplated objective (*OJ*), as shown in Equation (34).

$$OJ = OJ_{j} + Pen_{1}\sum_{NPQ}\Delta V_{LL}^{2} + Pen_{2}\sum_{Nq}\Delta Q_{GG}^{2} + Pen_{3}\sum_{N_f}\Delta S_{FF}^{2},\ j = 1, \ldots .m \tag{34}$$

where ΔV_{LL}, ΔQ_{GG}, and ΔS_{FF} are presented as:

$$\Delta V_{LL} = \begin{cases} V_{L}^{\min} - V_{L} & if\ V_{L} < V_{L}^{\min} \\ V_{L}^{max} - V_{L} & if\ V_{L} > V_{L}^{max} \end{cases} \tag{35}$$

$$\Delta Q_{GG} = \begin{cases} Q_{G}^{\min} - Q_{G} & if\ Q_{G} < Q_{G}^{\min} \\ Q_{G}^{max} - Q_{G} & if\ Q_{G} > Q_{G}^{max} \end{cases} \tag{36}$$

$$\Delta S_{FF} = S_{F}^{max} - S_{F}\ \ if\ S_{F} > S_{F}^{max} \tag{37}$$

Figure 2 displays the stages of the designed GTOT for OPFP in EPSs.

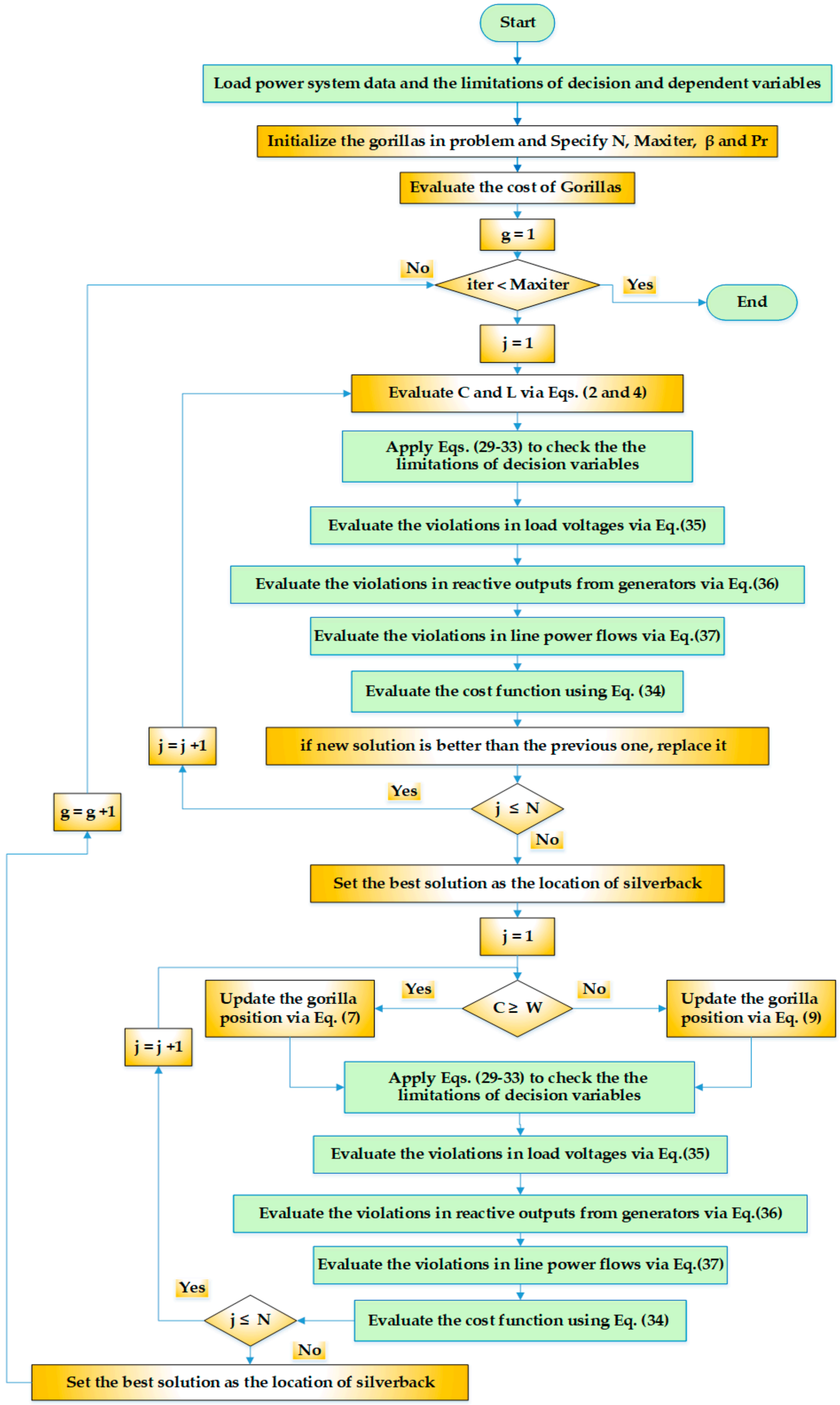

Figure 2. Developed solution-based GTOT for OPFP in EPSs.

On the other side, in order to handle the model of multi-objectives, the different objective functions can be augmented using the weighted sum approach as follows:

$$OJ = w_1 \frac{OJ_1}{OJ_{1max}} + w_2 \frac{OJ_2}{OJ_{2max}} + w_3 \frac{OJ_3}{OJ_{3max}} + w_4 \frac{OJ_4}{OJ_{4max}} \tag{38}$$

where

$$\sum_{i=1}^{4} w_i = 1 \tag{39}$$

5. Simulation Results

The developed GTOT is implemented on the standard IEEE 30-bus EPS, a practical Egyptian EPS called West Delta-EPS (WD-EPS). Thirty simulation runs are conducted based on the developed GTOT with peak iterations of 300 and gorillas' group of 25 members. The first EPS is depicted in Figure 3, which consists of 41 transmission lines, 30 buses, 4 tap changers, 6 generators, and 9 reactive power devices. The complete data of this EPS are extracted from [46]. The highest and minimum generator voltages are 1.1 and 0.95 p.u., respectively. The second EPS is described in Figure 4, which consists of 52 buses. The highest and lowest generator voltages are 1.06 and 0.94 p.u., respectively. The developed GTOT and various other innovative techniques were presented to minimize the fuel generation costs such as CST [47], SST, NBT [48], and ISHT. MatlabR2017b is utilized to carry out the simulations using CPU (2.5 GHz) Intel(R)-Core (TM) i7-7200U and 8 GB of RAM.

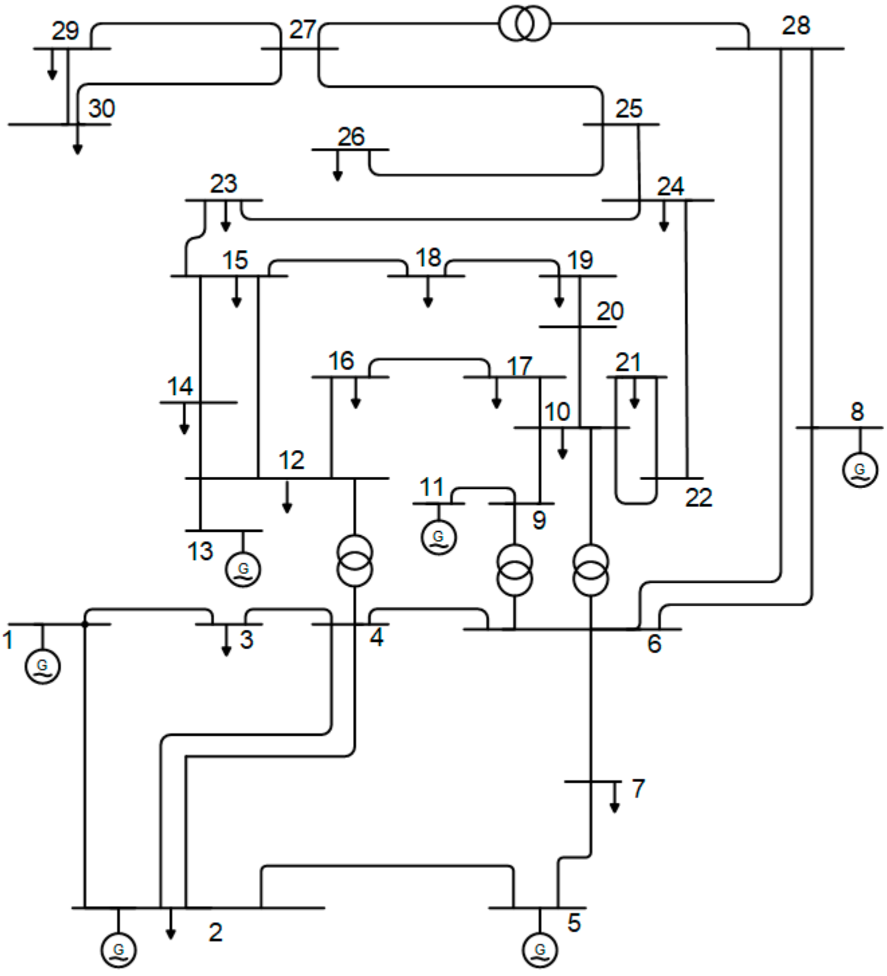

Figure 3. IEEE 30-bus EPS [42,49].

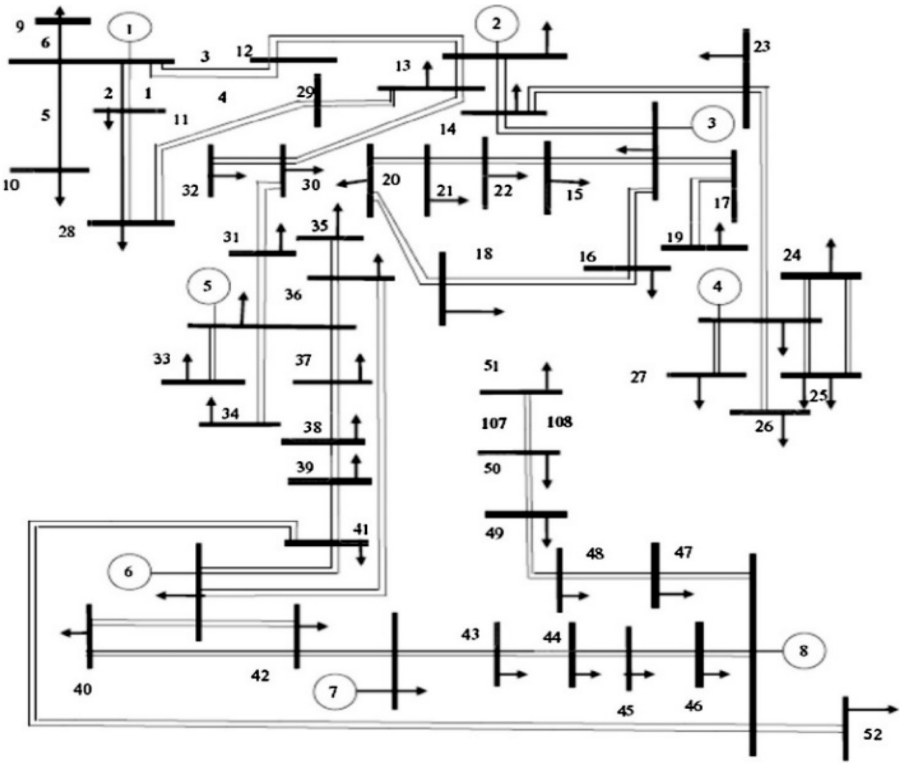

Figure 4. Real WD-EPS [50,51].

5.1. Results of the First EPS

For this EPS, six scenarios are examined:

- Scenario 1: OJ_1 minimization of FGCs described in Equation (16);
- Scenario 2: OJ_2 minimization of FGCSs described in Equation (17);
- Scenario 3: OJ_3 minimization of PE described in Equation (18);
- Scenario 4: OJ_4 minimization of OPL described in Equation (19);
- Scenario 5: Merging OJ_1 and OJ_3 as a multi-objective function;
- Scenario 6: Merging OJ_1, OJ_3, and OJ_4 as a multi-objective function.

5.1.1. Scenario 1

For this scenario, the proposed GTOT is implemented, and the results are shown in Table 1. In this table, the values of the voltages of the six generators (Vg_{1}, Vg_{2}, Vg_{5}, Vg_{8}, Vg_{11}, and Vg_{13}) started at 1.05, 1.04, 1.01, 1.01, 1.05, and 1.05, respectively, and ended at 1.1, 1.088, 1.0619, 1.0696, 1.1, and 1.0, respectively. In addition to this, the values of four tap changer settings ($Tap_{6\text{–}9}$, $Tap_{6\text{–}10}$, $Tap_{4\text{–}12}$, and $Tap_{28\text{–}27}$) started at 1.0780, 1.0690, 1.0320, and 1.0680, respectively, and ended at 1.0551, 0.90, 0.99, and 0.9669, respectively. Additionally, the values of all nine reactive power devices (Qc_{10}, Qc_{12}, Qc_{15}, Qc_{17}, Qc_{20}, Qc_{21}, Qc_{23}, Qc_{24}, and Qc_{29}) started at 0 and ended at 5.0, 5.0, 5.0, 5, 4.4549, 4.978, 2.7861, and 5.0, respectively. Furthermore, the values of all six generators' real power output (Pg_{1}, Pg_{2}, Pg_{5}, Pg_{8}, Pg_{11}, and Pg_{13}) started at 99.24, 80.0, 50.0, 20.0, 20.0, and 20.0, respectively, and ended at 177.0191, 48.7234, 21.2921, 21.0921, 11.8996, and 12.0, respectively. As demonstrated in this table, the proposed GTOT reduces FGCs from 901.96 USD/h to 799.0831 USD/h compared to the initial case. This decrease is a proportion of 11.406%. In addition, Figure 5 depicts the convergent characteristic of the proposed GTOT, where it obtains the optimal solution in a short time with the effectiveness and robustness of the solution.

Table 1. Simulation outcomes based on the designed GTOT for the first scenario.

Variables		Initial	First Scenario
Voltage setting of the generators (p.u)	**Gen $_1$**	1.0500	1.1000
	Gen $_2$	1.0400	1.0880
	Gen $_5$	1.0100	1.0619
	Gen $_8$	1.0100	1.0696
	Gen $_{11}$	1.0500	1.1000
	Gen $_{13}$	1.0500	1.1000
Output powers of the generators (MW)	**Gen $_1$**	99.2400	177.0191
	Gen $_2$	80.0000	48.7234
	Gen $_5$	50.0000	21.2921
	Gen $_8$	20.0000	21.0921
	Gen $_{11}$	20.0000	11.8995
	Gen $_{13}$	20.0000	12.0000
Tap setting of the transformers (p.u)	**Tr $_{6–9}$**	1.0780	1.0551
	Tr $_{6–10}$	1.0690	0.9000
	Tr $_{4–12}$	1.0320	0.9900
	Tr $_{28–27}$	1.0680	0.9668
Output reactive powers of the VAR sources ar buses (MVAr)	**Bus $_{10}$**	0.0000	5.0000
	Bus $_{12}$	0.0000	5.0000
	Bus $_{15}$	0.0000	5.0000
	Bus $_{17}$	0.0000	5.0000
	Bus $_{20}$	0.0000	4.4549
	Bus $_{21}$	0.0000	4.9780
	Bus $_{23}$	0.0000	2.7861
	Bus $_{24}$	0.0000	5.0000
	Bus $_{29}$	0.0000	2.6571
Cost_Pg		901.9600	799.0831
Losses		5.8324	8.6263

For this Scenario, Table 2 includes the comparison of reducing FGCs with a variety of other approaches. As shown, the developed GTOT obtains the minimum FGCs of 799.0831 USD/h, among other techniques.

Table 2. Comparison for Scenario 1.

Technique	FGCs (USD/h)	Technique	FGCs (USD/h)
Developed GTOT	799.0831	IMFT [52]	800.3848
GWT [53]	800.4330	SOST [54]	801.5733
TLT [27]	800.4212	ICT) [55]	801.843
GT [56]	800.9728	DHST [57]	802.2966
MCST [58]	799.3332	GA [41]	802.1962
BHBT [57]	799.9217	AGT [56]	800.0212
MST [59]	800.5099	CST [47]	799.8266
IEOT [60]	799.688	EMRFT [42]	798.9888
NBT [61]	799.7516	JFST [62]	799.1065

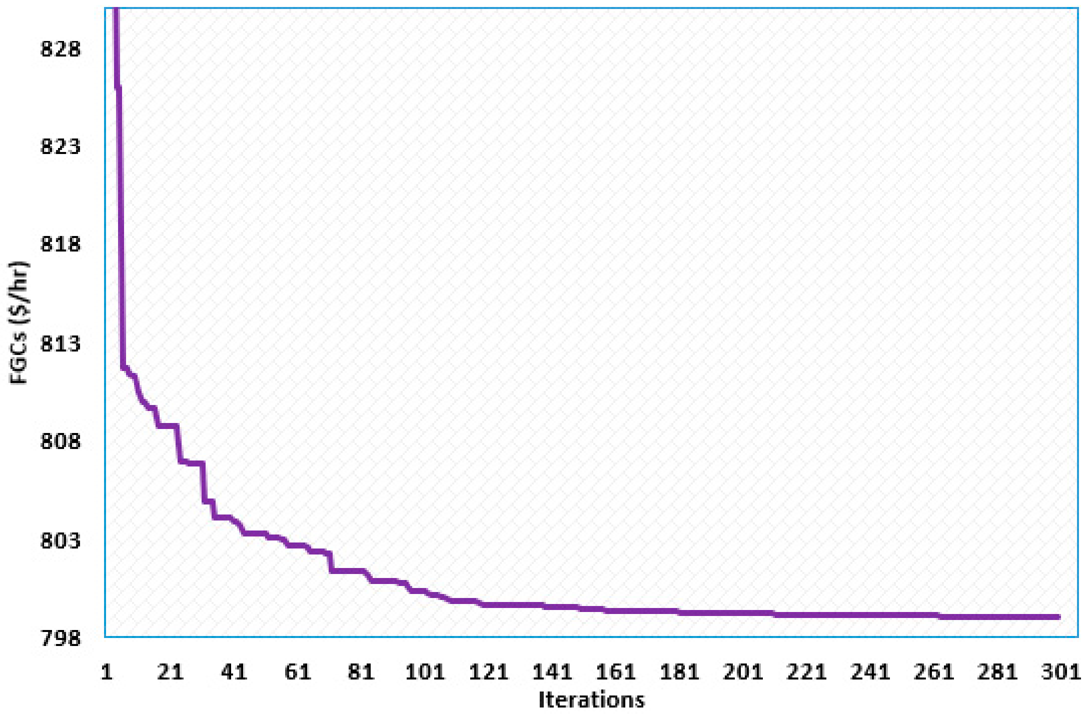

Figure 5. Convergence feature of developed GTOT for Scenario 1.

5.1.2. Scenario 2

Taking into account the valve point impact, the developed GTOT is used to reduce FGCSs. For this scenario, the regarding results are shown in Table 3. In this table, the values of the voltages of the six generators (Vg_{1}, Vg_{2}, Vg_{5}, Vg_{8}, Vg_{11}, and Vg_{13}) started at 1.050, 1.040, 1.010, 1.010, 1.050, and 1.050, respectively, and ended at 1.1000, 1.0809, 1.0550, 1.0653, 1.0999, and 1.1000, respectively. In addition to this, the values of four tap changer settings ($Tap_{6–9}$, $Tap_{6–10}$, $Tap_{4–12}$, and $Tap_{28–27}$) started at 1.0780, 1.0690, 1.0320, and 1.0680, respectively, and ended at 1.1000, 0.9203, 1.0595, and 0.9936, respectively. Additionally, the values of all nine reactive power devices (Qc_{10}, Qc_{12}, Qc_{15}, Qc_{17}, Qc_{20}, Qc_{21}, Qc_{23}, Qc_{24}, and Qc_{29}) started at 0 and ended at 5.0000, 4.994, 4.8523, 5.0000, 5.0000, 5.0000, 3.7342, 4.5993, and 2.8053, respectively. Furthermore, the values of all six generators' real power output (Pg_{1}, Pg_{2}, Pg_{5}, Pg_{8}, Pg_{11}, and Pg_{13}) started at 99.2400, 80.0000, 50.0000, 20.0000, 20.0000, and 20.0000, respectively, and ended at 194.7610, 47.7489, 19.0111, 10, 10.0000, and 12.0014, respectively. As shown, the developed GTOT reduces the FGCSs from 901.9600 USD/h in the initial scenario to 832.7696 USD/h in the final scenario. This reduction in cost represents a percentage of 7.6700%. Additionally, Figure 6 displays the convergent characteristic of the proposed GTOT, where it obtains the optimal solution in a short time with the effectiveness and robustness of the solution.

Table 3. Simulation outcomes based on the designed GTOT for the second scenario.

Variables		Initial	Second Scenario
Voltage setting of the generators (p.u)	**Gen $_{1}$**	1.0500	1.1000
	Gen $_{2}$	1.0400	1.0809
	Gen $_{5}$	1.0100	1.0550
	Gen $_{8}$	1.0100	1.0653
	Gen $_{11}$	1.0500	1.0999
	Gen $_{13}$	1.0500	1.1000

Table 3. *Cont.*

Variables		Initial	Second Scenario
Output powers of the generators (MW)	Gen_{1}	99.2400	194.7610
	Gen_{2}	80.0000	47.7489
	Gen_{5}	50.0000	19.0111
	Gen_{8}	20.0000	10.0000
	Gen_{11}	20.0000	10.0000
	Gen_{13}	20.0000	12.0014
Tap setting of the transformers (p.u)	$Tr_{6\text{–}9}$	1.0780	1.1000
	$Tr_{6\text{–}10}$	1.0690	0.9203
	$Tr_{4\text{–}12}$	1.0320	1.0595
	$Tr_{28\text{–}27}$	1.0680	0.9936
Output reactive powers of the VAR sources ar buses (MVAr)	Bus_{10}	0.0	5.0000
	Bus_{12}	0.0	4.9949
	Bus_{15}	0.0	4.8523
	Bus_{17}	0.0	5.0000
	Bus_{20}	0.0	5.0000
	Bus_{21}	0.0	5.0000
	Bus_{23}	0.0	3.7342
	Bus_{24}	0.0	4.5993
	Bus_{29}	0.0	2.8053
Cost_Pg		901.9600	832.7696
Losses		5.8324	10.1201

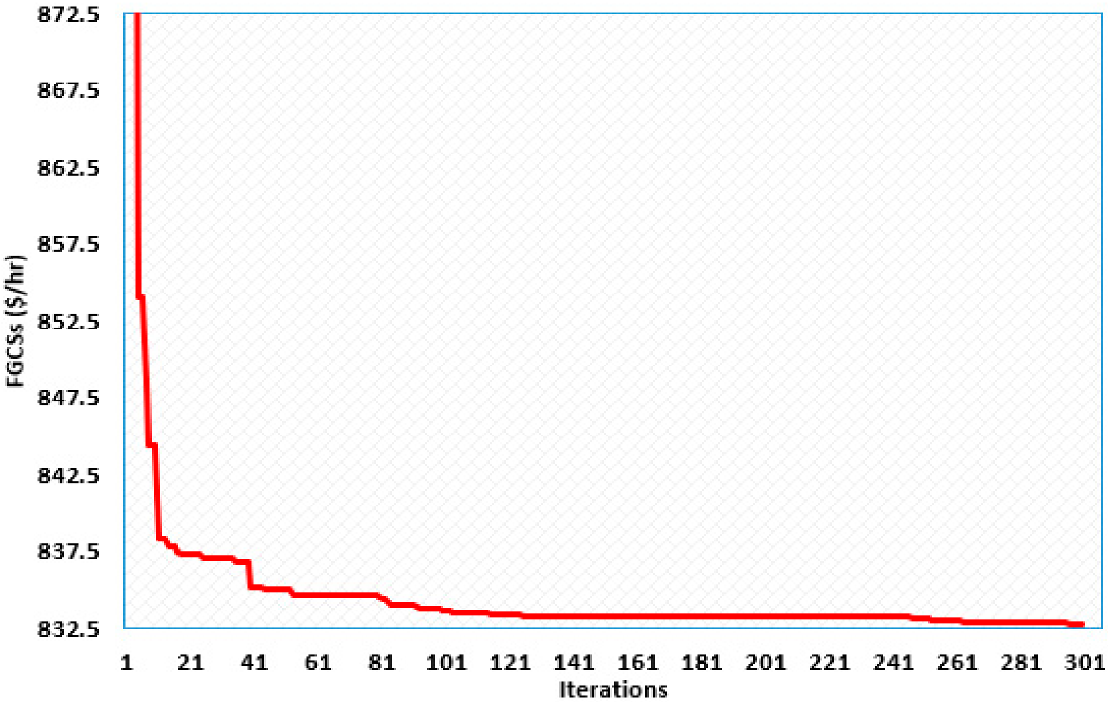

Figure 6. Convergence feature of the developed GTOT for Scenario 2.

5.1.3. Scenario 3

As demonstrated in Table 4, the designed GTOT minimizes the PEs in the third scenario. In this table, the values of the voltages of the six generators (Vg $_1$, Vg $_2$, Vg $_5$, Vg $_8$, Vg $_{11}$, and Vg $_{13}$) started at 1.0500, 1.0400, 1.0100, 1.0100, 1.0500, and 1.0500, respectively, and ended at 1.1000, 1.0961, 1.0784, 1.0859, 1.1000 and 1.1000, respectively.

Table 4. Simulation outcomes based on the designed GTOT for the third scenario.

Variables		Initial	Third Scenario
Voltage setting of the generators (p.u)	**Gen $_1$**	1.0500	1.1000
	Gen $_2$	1.0400	1.0961
	Gen $_5$	1.0100	1.0784
	Gen $_8$	1.0100	1.0859
	Gen $_{11}$	1.0500	1.1000
	Gen $_{13}$	1.0500	1.1000
Output powers of the generators (MW)	**Gen $_1$**	99.2400	63.9480
	Gen $_2$	80.0000	67.4323
	Gen $_5$	50.0000	50.0000
	Gen $_8$	20.0000	35.0000
	Gen $_{11}$	20.0000	30.0000
	Gen $_{13}$	20.0000	40.0000
Tap setting of the transformers (p.u)	**Tr $_{6\text{–}9}$**	1.0780	1.0696
	Tr $_{6\text{–}10}$	1.0690	0.9001
	Tr $_{4\text{–}12}$	1.0320	0.9864
	Tr $_{28\text{–}27}$	1.0680	0.9731
Output reactive powers of the VAR sources ar buses (MVAr)	**Bus $_{10}$**	0.0000	4.9999
	Bus $_{12}$	0.0000	4.9999
	Bus $_{15}$	0.0000	5.0000
	Bus $_{17}$	0.0000	5.0000
	Bus $_{20}$	0.0000	4.3098
	Bus $_{21}$	0.0000	4.9999
	Bus $_{23}$	0.0000	2.3956
	Bus $_{24}$	0.0000	5.0000
	Bus $_{29}$	0.0000	2.3154
Cost_Pg		901.9600	943.5287
Losses		5.8324	2.9803
Emissions		0.2390	0.2046

In addition to this, the values of four tap changer settings (Tap $_{6\text{–}9}$, Tap $_{6\text{–}10}$, Tap $_{4\text{–}12}$, and Tap $_{28\text{–}27}$) started at 1.0780, 1.0690, 1.0320, and 1.0680, respectively, and ended at 1.0696, 0.9001, 0.9864, and 0.9731, respectively. Additionally, the values of all nine reactive power devices (Qc $_{10}$, Qc $_{12}$, Qc $_{15}$, Qc $_{17}$, Qc $_{20}$, Qc $_{21}$, Qc $_{23}$, Qc $_{24}$, and Qc $_{29}$) started at zero and ended at 4.9999, 4.9999, 5.0000, 5, 4.3098, 4.9999, 2.3956, and 5.0000, respectively. Furthermore, the values of all six generators' real power output (Pg $_1$, Pg $_2$, Pg $_5$, Pg $_8$, Pg $_{11}$, and Pg $_{13}$) started at 99.2400, 80.0000, 50.0000, 20.0000, 20.0000, and 20.0000, respectively, and ended at 63.9480, 67.4323, 50.0000, 35.0000, 30.0000, and 40.0000, respectively. It is illustrated from this table that the obtained PE value is 0.2046 ton/h.

In addition to this, Figure 7 depicts the convergence properties of the generated GTOT for Scenario 3, where it obtains the optimal solution in a short time with the effectiveness and robustness of the solution. Table 5 compares it to other metaheuristics optimization techniques. It is illustrated from the table the developed GTOT attains the minimum PE objective of 0.2046 ton/h. It outperforms the other metaheuristics that are shown in the mentioned table.

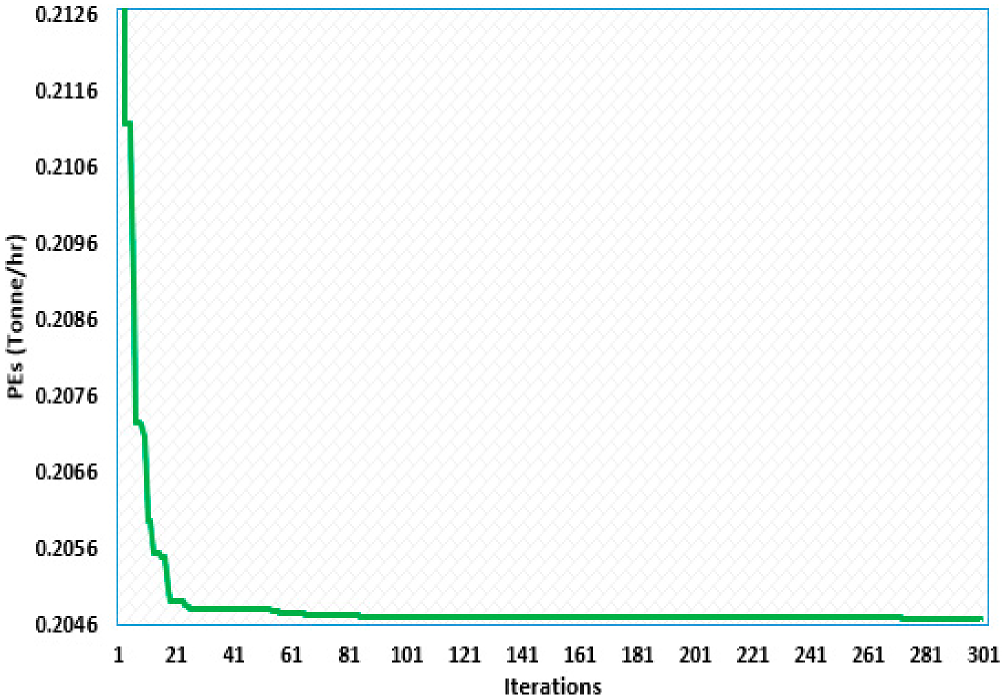

Figure 7. Convergence feature of the developed GTOT for Scenario 3.

Table 5. Comparison for Scenario 3.

Technique	PEs (tonne/h)	Technique	PEs (ton/h)
Developed GTOT	0.2046	AGT [56]	0.2048
Stud KHT [63]	0.2048	GT [56]	0.2049
ARBT [21]	0.2048	Modified TLT [64]	0.2049
KHT [63]	0.2049	EMRFT [42]	0.2048
CST [58]	0.2051	NBT [58]	0.2052
JFST [62]	0.2047	MCST [58]	0.2049

5.1.4. Scenario 4

The proposed GTOT achieves the minimizing of the OPLs in the fourth scenario, as shown in Table 6. In this table, the values of the voltages of the six generators (Vg_{1}, Vg_{2}, Vg_{5}, Vg_{8}, Vg_{11}, and Vg_{13}) started at 1.0500, 1.0400, 1.0100, 1.0100, 1.0500, and 1.0500, respectively, and ended at 1.1000, 1.0975, 1.0797, 1.0868, 1.1000, and 1.1000, respectively. In addition to this, the values of four tap changer settings ($Tap_{6\text{–}9}$, $Tap_{6\text{–}10}$, $Tap_{4\text{–}12}$, and $Tap_{28\text{–}27}$) started at 1.0780, 1.0690, 1.0320, and 1.0680, respectively, and ended at 1.0675, 0.9000, 0.9872, and 0.9728, respectively. Additionally, the values of all nine reactive power devices (Qc_{10}, Qc_{12}, Qc_{15}, Qc_{17}, Qc_{20}, Qc_{21}, Qc_{23}, Qc_{24}, and Qc_{29}) started at 0 and ended at 5.0000, 5.0000, 5.0000, 5.0000, 4.999, 5, 1.4887, 5.0000, and 2.2640, respectively. Furthermore, the values of all six generators' real power output (Pg_{1}, Pg_{2}, Pg_{5}, Pg_{8}, Pg_{11}, and Pg_{13}) started at 99.2400, 80.0000, 50.0000, 20.0000, 20.0000, and 20.0000, respectively, and ended at 51.2525, 80.0000, 50.0000, 35.0000, 30.0000, and 40.0000, respectively. It is illustrated from the table the acquired value of OPLs is 2.8525 MW, whereas the value of OPLs is 5.8324 MW in the initial scenario. This reduction in cost represents a percentage of 51.09%. Additionally, Figure 8 depicts the convergent characteristic of the designed GTOT for Scenario 4, where it obtains the optimal solution in a short time with the effectiveness and robustness of the solution.

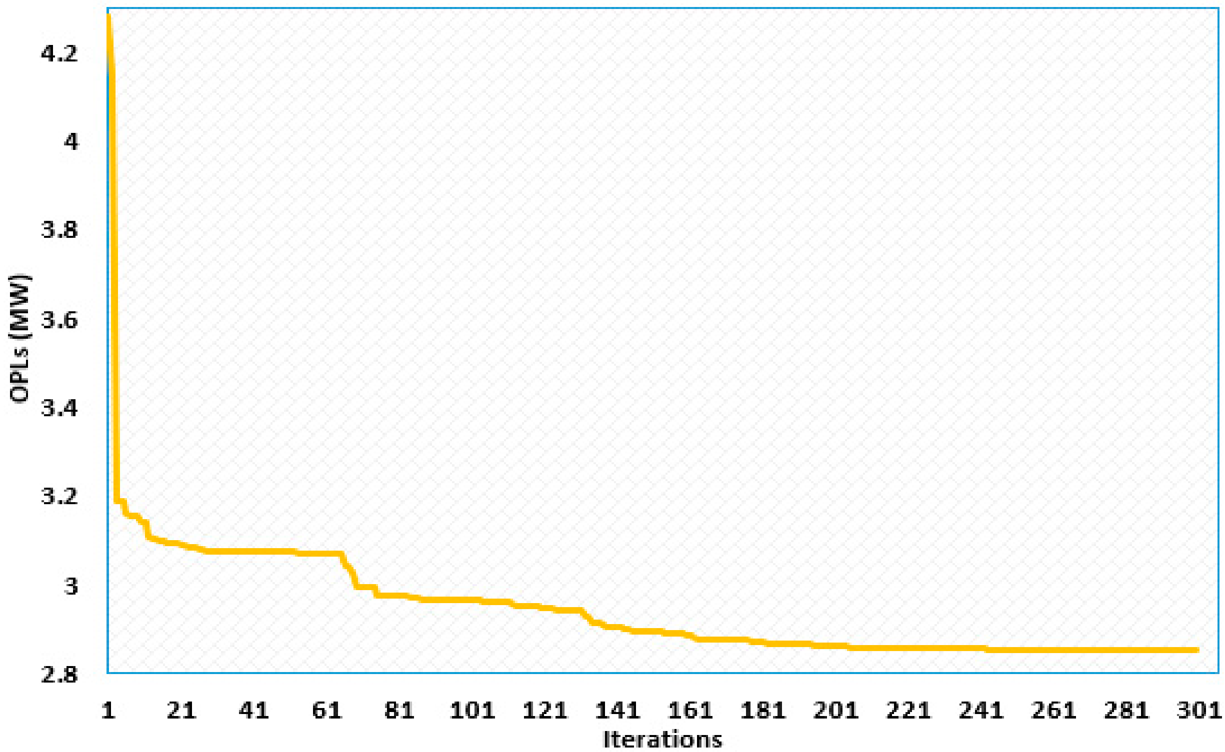

Figure 8. Convergence feature of the developed GTOT for Scenario 4.

Table 6. Simulation outcomes based on the designed GTOT for the fourth scenario.

Variables		Initial	Fourth Scenario
Voltage setting of the generators (p.u)	**Gen $_1$**	1.0500	1.1000
	Gen $_2$	1.0400	1.0975
	Gen $_5$	1.0100	1.0797
	Gen $_8$	1.0100	1.0868
	Gen $_{11}$	1.0500	1.1000
	Gen $_{13}$	1.0500	1.1000
Output powers of the generators (MW)	**Gen $_1$**	99.2400	51.2525
	Gen $_2$	80.0000	80.0000
	Gen $_5$	50.0000	50.000
	Gen $_8$	20.0000	35.0000
	Gen $_{11}$	20.0000	30.0000
	Gen $_{13}$	20.0000	40.0000
Tap setting of the transformers (p.u)	**Tr $_{6–9}$**	1.0780	1.0675
	Tr $_{6–10}$	1.0690	0.9000
	Tr $_{4–12}$	1.0320	0.9872
	Tr $_{28–27}$	1.0680	0.9728

Table 6. *Cont.*

Variables		Initial	Fourth Scenario
Output reactive powers of the VAR sources ar buses (MVAr)	**Bus $_{10}$**	0.0000	5.0000
	Bus $_{12}$	0.0000	5.0000
	Bus $_{15}$	0.0000	5.0000
	Bus $_{17}$	0.0000	5.0000
	Bus $_{20}$	0.0000	4.9999
	Bus $_{21}$	0.0000	5.0000
	Bus $_{23}$	0.0000	1.4887
	Bus $_{24}$	0.0000	5.0000
	Bus $_{29}$	0.0000	2.2640
Cost_Pg		901.9600	967.0722
Losses		5.8324	2.8525

5.1.5. Stability Assessment of the Developed GTOT for the First EPS

To make a detailed evaluation of the stability of the developed GTOT for the first EPS, the obtained objectives of the thirty runs are recorded. For each scenario, the related average objective is calculated, and a graph is plotted to describe the percentage of every objective value to $\mathrm{Ind}_{\mathrm{OJk}}$, so the closeness of every run compared to the mean can be described. Figure 9 describes the obtained indicators of the related objective percentages via the developed GTOT.

$$\mathrm{Ind}_{\mathrm{OJ_k}} = \frac{OJ_k}{\frac{1}{30}\sum\limits_{k=1}^{30} OJ_k}, k = 1, 2, \ldots m \tag{40}$$

As it can be observed from the figure, the developed GTOT always has the ability to find a close percentage to 100% where its mean is near to its minimum value. The highest percentage of the index is 100.085% in the first scenario, while it reached 101.1680% in the second scenario. For the third scenario, the maximum index percentage is 101.0400, while it reached 100.05% in the fourth scenario. This demonstrates the high stability of the developed GTOT for all scenarios. Additionally, Table 7 indicates the statistical data for the four scenarios. As manifested in this table, the best, mean, and worst values obtained by the developed GTOT are very close, which illustrates the robustness of the developed GTOT.

Table 7. Statistical data based on the designed GTOT for the 4 scenarios.

Statistical Indices	Scenario 1	Scenario 2	Scenario 3	Scenario 4
Best	799.0831	832.8144	0.2046	2.8525
Mean	799.2081	833.4394	0.2050	2.9128
Worst	799.8904	843.1896	0.2072	3.1655
Standard deviation	0.2140	1.8636	0.0008	0.0824
Standard error	0.0390	0.3402	0.0001	0.0150
∣Best-Worst∣	0.1010%	1.2458%	1.2350%	10.9711%
∣Mean-Worst∣	0.0853%	1.1698%	1.0667%	8.6738%
∣Best-Mean∣	0.0156%	0.0750%	0.1665%	2.1139%

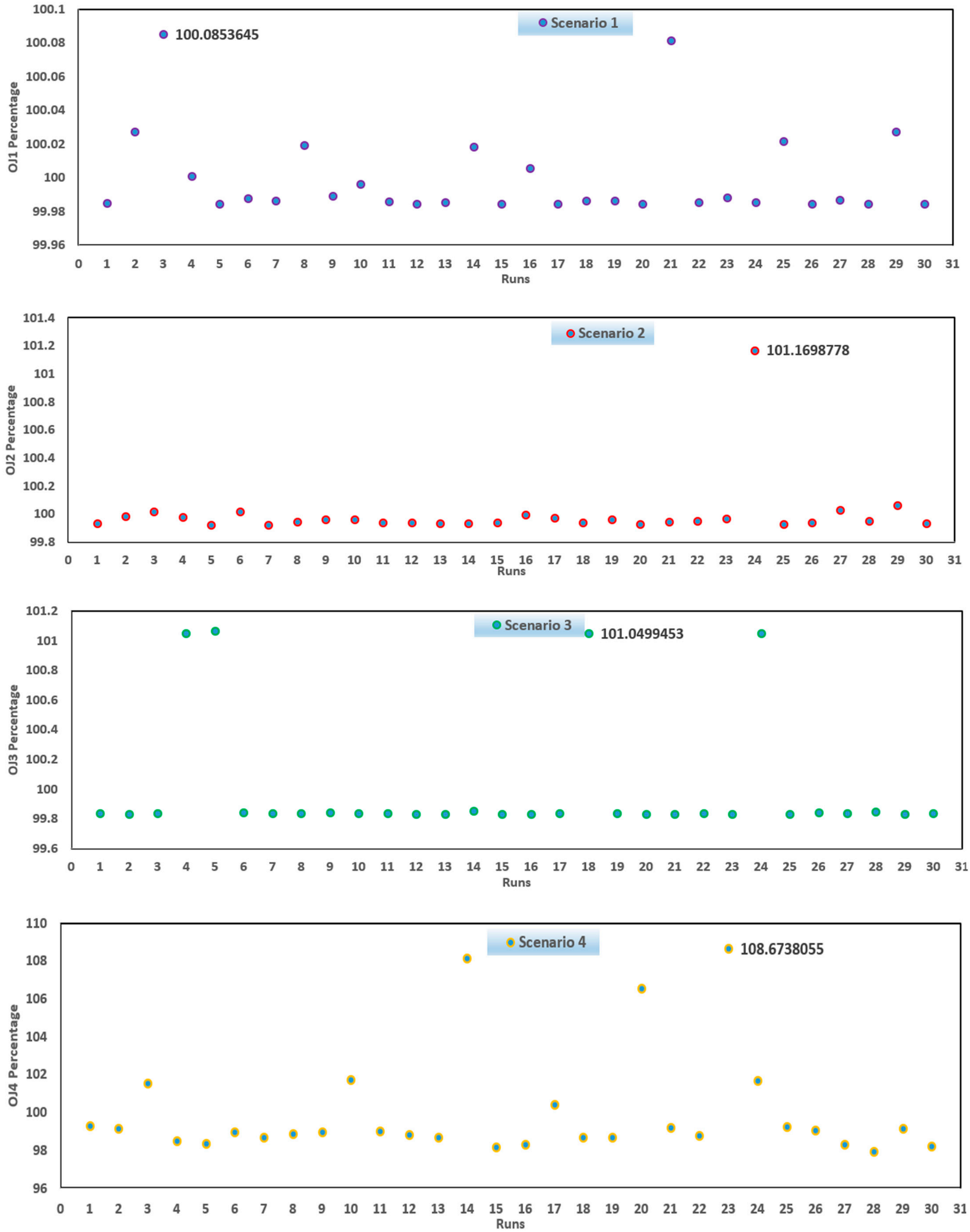

Figure 9. Obtained objectives percentages by means of the designed GTOT.

Moreover, other statistical indices are conducted on the four scenarios, which are standard deviation, standard error, ∣Best-Worst∣, ∣Mean-Worst∣, and ∣Best-Mean∣. The standard deviations for the four scenarios are 0.214, 1.8636, 0.0001, and 0.0150, while the standard errors are 0.0390, 0.3402, 0.0001, and 0.0150. Additionally, another important index, which is ∣Best-Mean∣, represents the difference between the best and mean values obtained by the proposed GTOT. The values of ∣Best-Mean∣ are 0.0156%, 0.0750%, 0.1665%, and 2.1139%. These statistical indices illustrate the effectiveness and robustness of the developed GTOT.

5.1.6. Scenario 5 and Scenario 6

In the fifth scenario, two different objective functions are considered for the minimization of both the FGCs and PE. In the sixth scenario, three different objective functions are considered for the minimization of FGCs, PE, and OPL. For both cases, the proposed GTOT is applied, and the optimal settings of the control variables and the regarding objectives are shown in Table 8. In this table, the values of FGCs and PE in the fifth scenario started at 901.9600 and 0.2390, respectively, and ended at 890.1029 and 0.2127, respectively, when applying the GTOT on this system. In addition to this, the values of FGCs, PE, and OPL in the sixth scenario started at 901.9600, 0.2390, and 5.8324, respectively, and ended at 895.4292, 0.2123, and 4.6529, respectively.

Table 8. Simulation outcomes based on the designed GTOT for the fifth and sixth scenario.

Variables		Initial	Fifth Scenario	Sixth Scenario
Voltage setting of the generators (p.u)	Gen $_{1}$	1.0500	1.1000	1.0057
	Gen $_{2}$	1.0400	1.0960	1.0045
	Gen $_{5}$	1.0100	1.0771	1.0003
	Gen $_{8}$	1.0100	1.0881	1.0111
	Gen $_{11}$	1.0500	1.1000	1.0007
	Gen $_{13}$	1.0500	1.0546	1.0018
Output powers of the generators (MW)	Gen $_{1}$	99.2400	1.0553	1.0137
	Gen $_{2}$	80.0000	1.1000	0.9097
	Gen $_{5}$	50.0000	1.1000	0.9814
	Gen $_{8}$	20.0000	1.1000	0.9741
	Gen $_{11}$	20.0000	6.243×10^{-9}	5.0000
	Gen $_{13}$	20.0000	0.0000	5.0000
Tap setting of the transformers (p.u)	Tr $_{6–9}$	1.0780	5.0000	5.0000
	Tr $_{6–10}$	1.0690	4.6221	5.0000
	Tr $_{4–12}$	1.0320	0.0000	5.0000
	Tr $_{28–27}$	1.0680	5.0000	5.0000
Output reactive powers of the VAR sources ar buses (MVAr)	Bus $_{10}$	0.0000	5.0000	5.0000
	Bus $_{12}$	0.0000	5.0000	5.0000
	Bus $_{15}$	0.0000	5.0000	4.9517
	Bus $_{17}$	0.0000	82.1327	81.8371
	Bus $_{20}$	0.0000	62.7968	62.4782
	Bus $_{21}$	0.0000	37.4611	38.7375
	Bus $_{23}$	0.0000	35.0000	35.0000
	Bus $_{24}$	0.0000	30.0000	30.0000
	Bus $_{29}$	0.0000	40.0000	40.0000

Table 8. *Cont.*

Variables	Initial	Fifth Scenario	Sixth Scenario
Cost_Pg	901.9600	890.1029	895.4292
Losses	5.8324	3.9906	4.6529
Emissions	0.2390	0.2127	0.2123
Fitness	1.0000	0.7705	0.6691

Additionally, Table 9 indicates the statistical data for the fifth and sixth scenarios. As manifested in this table, the best, mean, and worst values obtained by the developed GTOT are very close, which illustrates the robustness of the developed GTOT. Moreover, other statistical indices are conducted on the four scenarios, which are standard deviation, standard error, ∣Best-Worst∣, ∣Mean-Worst∣, and ∣Best-Mean∣, that illustrate the effectiveness and robustness of the developed GTOT.

Table 9. Simulation outcomes of the designed GTOT for the fifth and sixth scenario.

Statistical Indices	Scenario 5	Scenario 6
Best	0.7705	0.6691
Mean	0.7819	0.6896
Worst	0.7914	0.7473
Standard deviation	0.0909	0.0043
Standard error	0.0166	0.0008
∣Best-Worst∣	2.7057%	11.6914%
∣Mean-Worst∣	1.2176%	8.3600%
∣Best-Mean∣	1.4701%	3.0743%

Additionally, Table 9 indicates the statistical data for the fifth and sixth scenarios. As manifested in this table, the standard deviations for the four scenarios are 0.0909 and 0.0043, while the standard errors are 0.0166 and 0.0008. Additionally, the values of ∣Best-Mean∣ obtained by the proposed GTOT are 1.4701% and 3.0743%. These statistical indices illustrate the effectiveness and robustness of the developed GTOT.

5.2. Results of the Second EPS

For this EPS, the three scenarios listed below are studied:

- Scenario 7: OJ_1 minimization described in Equation (16);
- Scenario 8: OJ_4 minimization described in Equation (19);
- Scenario 9: Merging OJ_1 and OJ_4 as a multi-objective function.

5.2.1. Scenario 7

For this case, the designed GTOT is implemented, and the results are shown in Table 10. In this table, the values of the voltages of the eight generators (Vg_1, Vg_2, Vg_3, Vg_4, Vg_5, Vg_6, Vg_7, and Vg_8) started at 1 and ended at 1.0600, 1.0590, 1.0599, 1.0599, 1.0599, 1.0599, 1.0455, and 1.0517, respectively. In addition to this, the values of all eight generators' real power output (Pg_1, Pg_2, Pg_3, Pg_4, Pg_5, Vg_6, Pg_7, and Pg_8) started at 85.6900, 157.4000, 139.3100, 113.6900, 166.4800, 31.7100, 92.000, and 122.4900, respectively, and ended at 189.5676, 10.0000, 214.6980, 180.4253, 10.0000, 234.0139, 56.3042, and 32.1957, respectively. As illustrated, the proposed GTOT reduces FGCs from 25,098.7000 USD/h to 22,953.42472 USD/h in comparison with the initial scenario. This decrease is a percentage of 8.54%. Furthermore, Figure 10 depicts the convergent characteristic of the proposed GTOT, where it obtains the optimal solution in a short time with the effectiveness and robustness of the solution.

Table 10. Simulation outcomes based on the designed GTOT for the seventh scenario.

Variables		Initial	Fifth Scenario
Voltage setting of the generators (p.u)	**Gen 1**	1.0000	1.0600
	Gen 2	1.0000	1.0599
	Gen 3	1.0000	1.0599
	Gen 4	1.0000	1.0599
	Gen 5	1.0000	1.0599
	Gen 6	1.0000	1.0599
	Gen 7	1.0000	1.0455
	Gen 8	1.0000	1.05173
Output powers of the generators (MW)	**Gen 1**	85.6900	189.5676
	Gen 2	157.400	10.0000
	Gen 3	139.3100	214.6980
	Gen 4	113.6900	180.4253
	Gen 5	166.4800	10.0000
	Gen 6	31.7100	234.0139
	Gen 7	92.0000	56.3042
	Gen 8	122.4900	32.1957
FGCs (USD/h)		**25,098.7000**	22,953.4247
OPLs (MW)		**19.0150**	37.4550

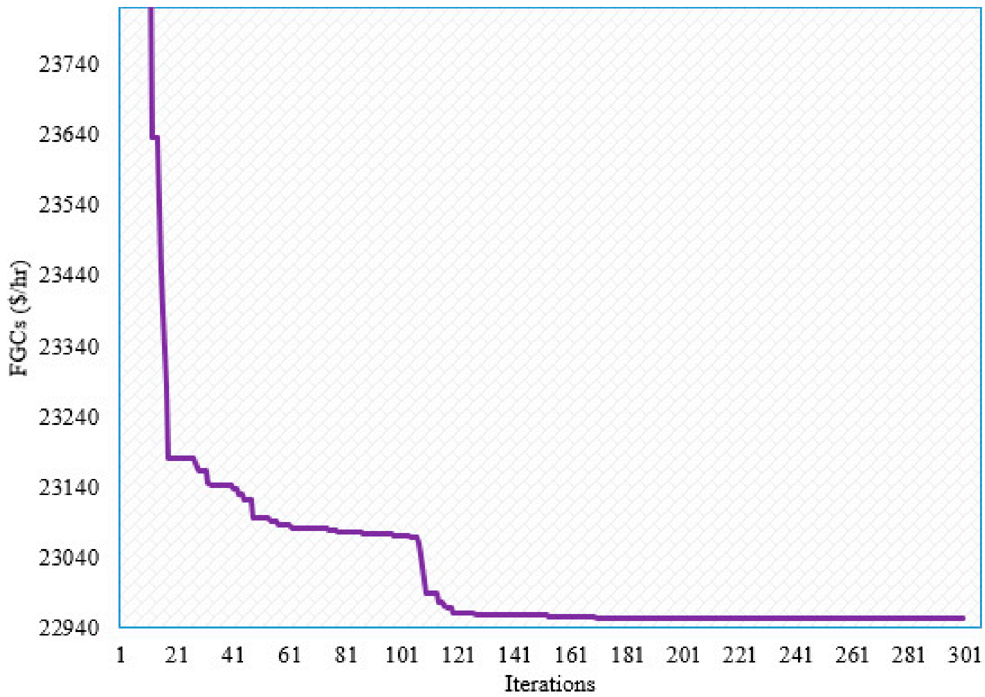

Figure 10. Convergence feature of developed GTOT for Scenario 7.

For such a scenario, the created GTOT is contrasted to a number of other novel approaches used in this instance, as shown in Table 11. As can be observed, the produced GTOT beats all other strategies in terms of minimizing FGCs, with the developed GTOT obtaining the smallest FGCs of 22,953.4247 USD/h.

Table 11. Comparison for Scenario 7.

Technique	FGCs (USD/h)	Technique	FGCs (USD/h)
Developed GTOT	22,953.4247	ISHT [65]	22,958.7800
NBT [48]	22,960.8100	CST [47]	22,959.3600
SST [65]	22,965.5900	MCST [47]	22,955.5500
GWT [65]	22,957.7200		

5.2.2. Scenario 8

The proposed GTOT achieves the minimizing of the OPLs in the eighth scenario, as shown in Table 12. In this table, the values of the voltages of the eight generators (Vg_1, Vg_2, Vg_3, Vg_4, Vg_5, Vg_6, Vg_7, and Vg_8) started at 1 and ended at 1.0595, 1.0600, 1.0600, 1.0600, 1.0600, 1.0600, 1.0600, and 1.0600, respectively. In addition to this, the values of all eight generators' real power output (Pg_1, Pg_2, Pg_3, Pg_4, Pg_5, Vg_6, Pg_7, and Pg_8) started at 85.6900, 157.4000, 139.3100, 113.6900, 166.4800, 31.7100, 92.0000, and 122.4900, respectively, and ended at 60.4617, 58.8194, 180.6455, 130.7554, 117.9838, 105.4722, 156.5709, and 86.2761, respectively. The proposed GTOT, as demonstrated, reduces the OPLs from 19.0150 MW to 7.2353 MW compared with the initial scenario. This decrease reflects a 61.95 percent reduction. In addition, Figure 11 depicts the related convergent characteristic of the proposed GTOT for Scenario 8, where it obtains the optimal solution in a short time with the effectiveness and robustness of the solution.

Table 12. Simulation outcomes based on the designed GTOT for the eighth scenario.

Variables		Initial	Sixth Scenario
Voltage setting of the generators (p.u)	**Gen $_1$**	1.0000	1.0595
	Gen $_2$	1.0000	1.0600
	Gen $_3$	1.0000	1.0600
	Gen $_4$	1.0000	1.0600
	Gen $_5$	1.0000	1.0600
	Gen $_6$	1.0000	1.0600
	Gen $_7$	1.0000	1.0600
	Gen $_8$	1.0000	1.0600
Output powers of the generators (MW)	**Gen $_1$**	85.6900	60.4617
	Gen $_2$	157.4000	58.8194
	Gen $_3$	139.3100	180.6455
	Gen $_4$	113.6900	130.7554
	Gen $_5$	166.4800	117.9838
	Gen $_6$	31.7100	105.4722
	Gen $_7$	92.0000	156.5709
	Gen $_8$	122.4900	86.2761
FGCs (USD/h)		**25,098.7000**	24,773.0865
OPLs (MW)		**19.0150**	7.2353

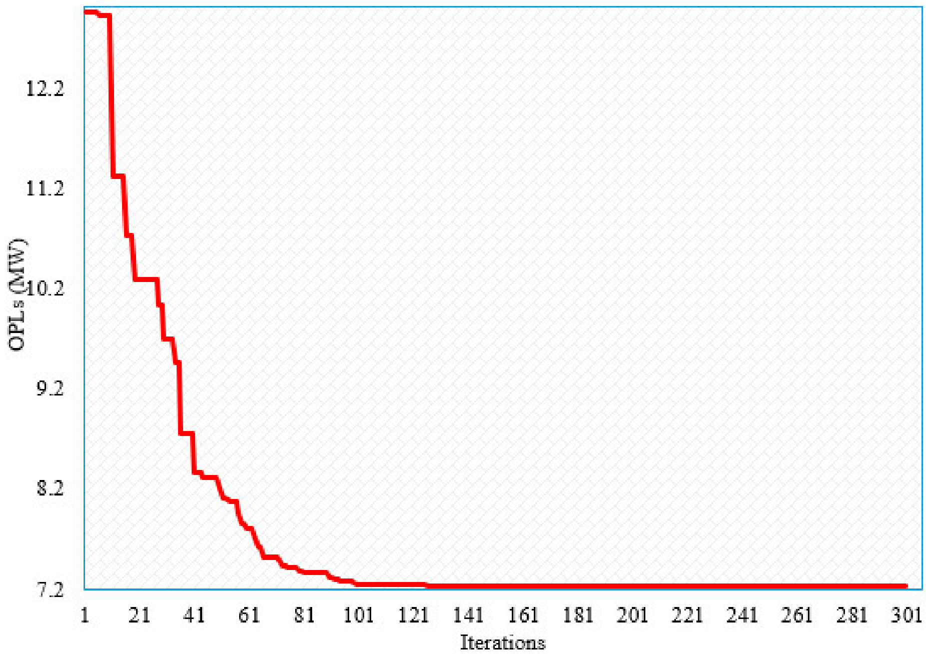

Figure 11. Convergence feature of the developed GTOT for Scenario 8.

5.2.3. Stability Assessment of the GTOT for the Second EPS

For this EPS, similarly, the obtained objectives of the thirty runs are recorded. For every scenario, the estimated indicators of the percentages of the objectives via the proposed GTOT are displayed in Figure 12.

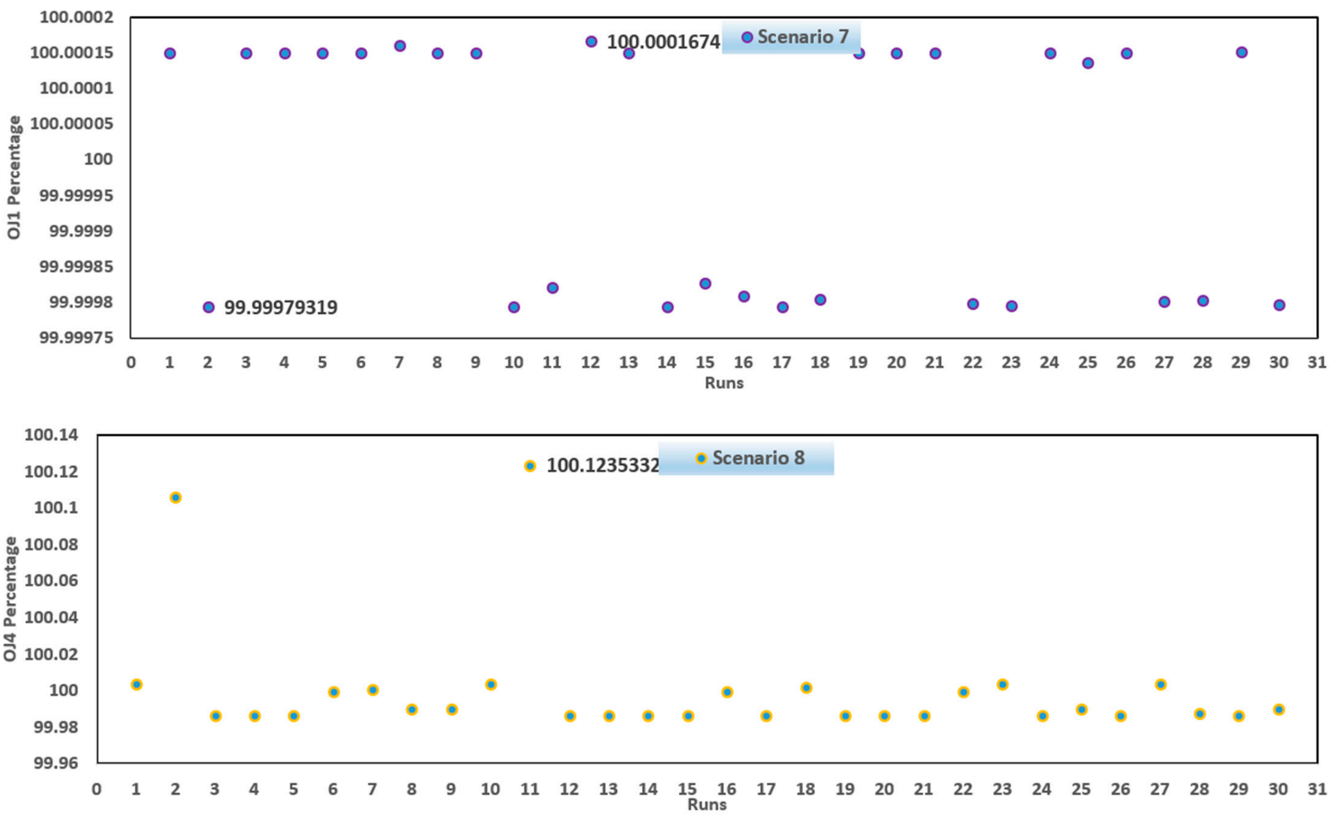

Figure 12. Estimated objective percentages via the designed GTOT.

As seen, the developed GTOT always has the ability to find close percentage to 100% where its mean is near to its minimum. For the first scenario, the highest indicator percent is 100.0000167%, while the minimum index percent is 99.9999%. The maximum index percent is 100.123%, while the minimum index percent is 99.9862%. This demonstrates the high stability of the developed GTOT for all scenarios.

Additionally, Table 13 indicates the statistical data for the seventh and eighth scenario. As manifested in this table, the standard deviations for the two scenarios are 7.3505 and 1.28×10^{-5} while the standard errors are 1.3420 and 2.33×10^{-6}. Additionally, the values of ∣Best-Mean∣ obtained by the proposed GTOT are 0.0137% and 0.0002%. These statistical indices illustrate the effectiveness and robustness of the developed GTOT.

Table 13. Simulation outcomes based on the GTOT for the seventh and eighth scenarios.

Statistical Indices	Scenario 7	Scenario 8
Best	22,953.4200	7.2353
Mean	22,956.5800	7.2353
Worst	22,984.9400	7.2353
Standard deviation	7.3505	1.28×10^{-5}
Standard error	1.3420	2.33×10^{-6}
∣Best-Worst∣	0.1373%	0.0003%
∣Mean-Worst∣	0.1235%	0.0001%
∣Best-Mean∣	0.0137%	0.0002%

5.2.4. Scenario 9

The designed GTOT achieves the minimization of both the FGCs and OPL in the ninth scenario, as shown in Table 14. In this table, the values of FGCs and OPL in the ninth scenario have started with 25,098.7000 and 19.0150, respectively, and ended with 24,586.3700 and 7.3036, respectively.

Table 14. Simulation outcomes based on the designed GTOT for Scenario 9.

Variables		Initial	Ninth Scenario
Voltage setting of the generators (p.u)	Gen $_1$	1.0000	1.0600
	Gen $_2$	1.0000	1.0600
	Gen $_3$	1.0000	1.0600
	Gen $_4$	1.0000	1.0600
	Gen $_5$	1.0000	1.0599
	Gen $_6$	1.0000	1.0600
	Gen $_7$	1.0000	1.0599
	Gen $_8$	1.0000	1.0600
Output powers of the generators (MW)	Gen $_1$	85.6900	67.2453
	Gen $_2$	157.4000	51.3626
	Gen $_3$	139.3100	183.2907
	Gen $_4$	113.6900	133.4820
	Gen $_5$	166.4800	108.3223
	Gen $_6$	31.7100	123.8325
	Gen $_7$	92.0000	148.2581
	Gen $_8$	122.4900	81.2601
FGCs (USD/h)		25,098.7000	24,586.3700
OPLs (MW)		19.0150	7.3036
Fitness		1.0000	0.6818

In addition, Figure 13 depicts the convergent characteristic of the designed GTOT for Scenario 9, where it obtains the optimal solution in a short time with the effectiveness and robustness of the solution. Moreover, Table 15 indicates the statistical data for the ninth scenario. As manifested in this table, the standard deviation for this scenario is 1.9551×10^{-8}, while the standard error is 3.5696×10^{-9}. Additionally, the value of ∣Best-Mean∣ obtained by the proposed GTOT is 3.4413×10^{-6}%. These statistical indices illustrate the effectiveness and robustness of the developed GTOT.

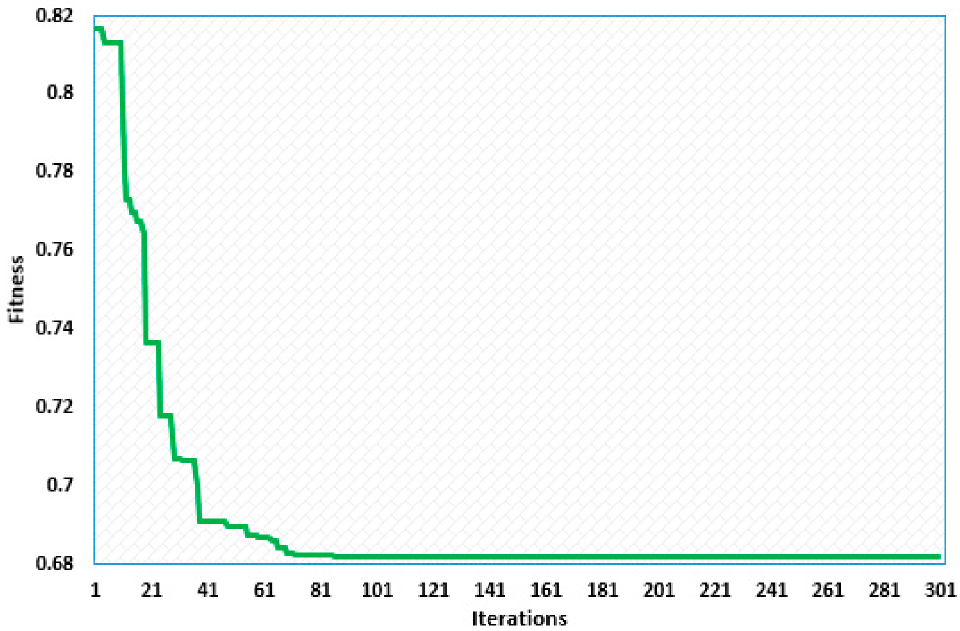

Figure 13. Convergence feature of the developed GTOT for Scenario 9.

Table 15. Simulation outcomes based on the designed GTOT for the seventh and eighth scenario.

Statistical Indices	Scenario 9
Best	0.6818
Mean	0.6818
Worst	0.6818
Standard deviation	1.9551×10^{-8}
Standard error	3.5696×10^{-9}
∣Best-Worst∣	6.1814×10^{-6}%
∣Mean-Worst∣	2.7401×10^{-6}%
∣Best-Mean∣	3.4413×10^{-6}%

6. Conclusions

In this paper, a methodology centered on the gorilla troops optimization technique (GTOT) is developed for optimal power flow problem (OPFP) in electrical power systems (EPSs). The assessment of the designed GTOT is carried out utilizing an IEEE specified 30 bus EPS and actual WD-EPS from Egypt. Nine different scenarios are evaluated, each with a different goal function of fuel expense, transmission losses, and harmful pollutants. Significant decreases in the objective goals are achieved for all tested circumstances. The main outcomes of this paper are developed as follows:

- Multi-dimension objectives combining two and three objectives for both systems are developed in this work.

- Their percentages of reduction for the single objectives are reached (11.406%, 7.67%, 14.39%, 51.09%, 8.54%, and 61.95%) for the six single objective scenarios in comparison to the initial circumstance.
- The GTOT is employed in different evaluations and statistical analyses with many modern methods such as GWT, CST, SST, NBT, and ISHT.
- The developed GTOT always has the ability to find a close percentage to 100% where its average is near to its minimum for both EPSs.
- When developed GTOT compared to other similar approaches in the literature, the simulated results demonstrate the designed GTOT's solution validity and stability.
- The developed GTOT derives considerable stability for all scenarios.

Considering the high efficacy of the suggested algorithm in the OPFP application in this paper, it is preferred that the proposed algorithm be tested in the future for resolving the OPFP with high penetration of renewable energies in power grids. It may also be designed for AC-DC electrical systems with the incorporation of modern voltage source converters.

Author Contributions: Conceptualization, A.G. and R.E.-S.; Data curation, A.S. and A.E.; Formal analysis, A.S., R.E.-S., A.E. and H.T.D.; Funding acquisition, E.E.; Investigation, R.E.-S. and A.E.; Methodology, A.G.; Resources, A.G., E.E. and H.T.D.; Software, A.S.; Supervision, R.E.-S. and H.T.D. All authors have read and agreed to the published version of the manuscript.

Funding: Taif University Researchers Supporting Project number (TURSP-2020/86), Taif University, Taif, Saudi Arabia.

Informed Consent Statement: Not applicable.

Data Availability Statement: Not applicable.

Conflicts of Interest: The authors declare no conflict of interest.

List of Acronyms

AGT	Adaptive GT
ARBT	Adaptive real biogeography-based technique
AGST	Adaptive group search technique
BBO	Biogeography-based optimization
BHBT	Black-hole-based technique
CBOA	Colliding bodies optimization algorithm
COA	Coyote optimization algorithm
CSSO	Chaotic salp swarm optimizer
CST	Crow search technique
DE	Differential evolution
DHST	Differential harmony search technique
EMM	Electromagnetism-like mechanism
EPSs	Electrical power systems
EMRFT	Enhanced manta ray foraging technique
EMSA	Emended moth swarm algorithm
FGCs	Fuel generation costs
FGCSs	FGC with sinusoids
GA	Genetic algorithm
GTOT	Gorilla troops optimization technique
GT	Grasshopper technique
GWT	Grey wolf technique
HGWODE	Hybridization of GWT and DE
ICT	Imperialist competitive technique
IEOT	Improved electromagnetism-like technique
IMFT	Improved moth-flame technique
INSGA-III	Improved non-dominated sorting genetic algorithm
ISHT	Improved spotted-hyena technique

ISST	Improved social spider technique
IADE	Adaptive differential evolution
JFST	Jellyfish search technique
KHT	Krill herd technique
MCST	Modified crow search technique
NBT	Novel bat technique
MRFT	Manta-ray foraging technique
MST	Moth swarm technique
OPFP	Optimal power flow problem
OPL	Overall power loss
PE	Produced emissions
PSO	Particle swarm optimization
QCMFT	Quantum computing and moth flame technique
SAO	Simulated annealing optimization
SOST	Symbiotic organisms search technique
SST	Salp swarm technique
TLT	Teaching-learning technique
WCEMFT	Combination of water cycle with moth flame technique
WD	West delta
WD-EPS	West Delta-EPS

List of Variables

A	Level of violence in a fight
Xr	The current group position of gorilla
LL	Variables' minimum bound
$X(g)$	Vector of gorilla location in the g iteration
$GX(g+1)$	Vector of gorilla location in the $g+1$ iteration
$rand$, $rd1$, $rd2$, $rd3$	Random values ranging from 0 to 1
Pr	Migrating coefficient
GXr	Candidate group position of gorilla
UL	Variables' maximum bound
$Iter$	Present iteration number
$MaxIter$	Maximum iteration number
$rd4$	Random value inside the bound [0:1]
l	Random values between -1 and 1
$X(g)$	Vector of gorilla location
Q	Force of impact
$rd5$	Random value within bound [0:1]
β	Pre-optimization value
E	Violence efficacy
$Vg_1, Vg_2, \ldots, Vg_{Ng})$	Voltages of the generators
$Tap_1, Tap_2, \ldots\ Tap_{Nt}$	Tap changer settings
Nt	Number of on-load tap changers
$Qg_1, Qg_2, \ldots, Qg_{Ng}$	Generator reactive power outputs
$Pg_1, Pg_2, \ldots, Pg_{Ng}$	Generators' real power output
OJ	Investigated vector of several m targets
OJ_1	Costs of fuel generation in dollars per hour
Pg_k	Real power output in megawatts of generator
OJ_2	Costs of fuel generation with sinusoids
θ	Phase angle
G_{mn}	Conductance of a line between buses m and n
QL	Power consumption in its reactive components
G_{jk}	Mutual conductance of line between bus j and k
VL_j	Load voltage at bus j
OJ_j	Each objective function
NRA	Newton–Raphson approach

Pen_3	Penalty coefficient for any violation in line flow
Ng	Number of on-load generators
Nq	Number of on-load reactive power sources,
$SF_1, \ldots, SF_{NF}$	Transmission flow limits
Z	Random values between [−c:c]
$X_{silverback}$	The best solution which is the silverback
N	Population of gorillas
A	Level of violence in a fight
$VL_1, \ldots, VL_{NPQ}$	Load bus voltage magnitudes
NPQ	The number of load buses,
x	Independent variables
y	Dependent variables
m	Vector of several targets
k; C_k, B_k, and A_k	Cost factors of generator k
NF	Number of transmission lines
$Qc_1, Qc_2, \ldots, Qc_{Nq}$	Reactive power injections of switching capacitors
$Pg_k^{\min}$	Lowest limitation of generator k
E_k and F_k	Generator k's sinusoid cost factors
OJ_3	Produced ton/hr emissions from the power plants
γ_k, β_k, α_k, ξ_k, and λ_k	Emission factors of generator k
Nb	Number of buses
V	Voltage
PL	Power consumption in its active components
B_{jk}	Mutual susceptance of a line between bus j and k
S_{fl}	Power flow via line
Pen_1	Penalty coefficient for violation in load voltage
Pen_2	Penalty coefficient for violation in reactive power output from generators
$\mathrm{Ind}_{\mathrm{OJk}}$	Mean value

References

1. Trivedi, I.N.; Jangir, P.; Parmar, S.A.; Jangir, N. Optimal Power Flow with Voltage Stability Improvement and Loss Reduction in Power System Using Moth-Flame Optimizer. *Neural Comput. Appl.* **2018**, *30*, 1889–1904. [CrossRef]
2. Buch, H.; Trivedi, I.N.; Jangir, P. Moth Flame Optimization to Solve Optimal Power Flow with Non-Parametric Statistical Evaluation Validation. *Cogent Eng.* **2017**, *4*, 1286731. [CrossRef]
3. Attia, A.F.; El Sehiemy, R.A.; Hasanien, H.M. Optimal Power Flow Solution in Power Systems Using a Novel Sine-Cosine Algorithm. *Int. J. Electr. Power Energy Syst.* **2018**, *99*, 331–343. [CrossRef]
4. Montoya, O.D. A Convex OPF Approximation for Selecting the Best Candidate Nodes for Optimal Location of Power Sources on DC Resistive Networks. *Eng. Sci. Technol. Int. J.* **2020**, *23*, 527–533. [CrossRef]
5. Bai, X.; Wei, H. A Semidefinite Programming Method with Graph Partitioning Technique for Optimal Power Flow Problems. *Int. J. Electr. Power Energy Syst.* **2011**, *33*, 1309–1314. [CrossRef]
6. Dommel, H.W.; Tinney, W.F. Optimal Power Flow Solutions. *IEEE Trans. Power Appar. Syst.* **1968**, *PAS-87*, 1866–1876. [CrossRef]
7. Crisan, O.; Mohtadi, M.A. Efficient Identification of Binding Inequality Constraints in the Optimal Power Flow Newton Approach. *IEE Proc. C Gener. Transm. Distrib.* **1992**, *139*, 365–370. [CrossRef]
8. Mota-Palomino, R.; Quintana, V.H. Sparse Reactive Power Scheduling by a Penalty Function-Linear Programming Technique. *IEEE Trans. Power Syst.* **1986**, *1*, 31–39. [CrossRef]
9. Granelli, G.P.; Montagna, M. Security-Constrained Economic Dispatch Using Dual Quadratic Programming. *Electr. Power Syst. Res.* **2000**, *56*, 71–80. [CrossRef]
10. Burchett, R.C.; Happ, H.H.; Vierath, D.R. Quadratically Convergent Optimal Power Flow. *IEEE Trans. Power Appar. Syst.* **1984**, *PAS-103*, 3267–3275. [CrossRef]
11. El-Sehiemy, R.A.; El Ela, A.A.A.; Shaheen, A. A Multi-Objective Fuzzy-Based Procedure for Reactive Power-Based Preventive Emergency Strategy. *Int. J. Eng. Res. Afr.* **2015**, *13*, 91–102. [CrossRef]
12. Rahli, M.; Pirotte, P. Optimal Load Flow Using Sequential Unconstrained Minimization Technique (SUMT) Method under Power Transmission Losses Minimization. *Electr. Power Syst. Res.* **1999**, *52*, 61–64. [CrossRef]
13. Sun, D.I.; Ashley, B.; Brewer, B.; Hughes, A.; Tinney, W.F. Optimal Power Flow by Newton Approach. *IEEE Trans. Power Appar. Syst.* **1984**, *PAS-103*, 2864–2880. [CrossRef]
14. Santos, A.; da Costa, G.R.M. Optimal-Power-Flow Solution by Newton's Method Applied to an Augmented Lagrangian Function. *IEE Proc. Gener. Transm. Distrib.* **1995**, *142*, 33–36. [CrossRef]

15. Yan, X.; Quintana, V.H. Improving an Interior-Point-Based off by Dynamic Adjustments of Step Sizes and Tolerances. *IEEE Trans. Power Syst.* **1999**, *14*, 709–716. [CrossRef]
16. Yan, W.; Yu, J.; Yu, D.C.; Bhattarai, K. A New Optimal Reactive Power Flow Model in Rectangular Form and Its Solution by Predictor Corrector Primal Dual Interior Point Method. *IEEE Trans. Power Syst.* **2006**, *21*, 61–67. [CrossRef]
17. Momoh, J.A.; Zhu, J.Z. Improved Interior Point Method for off Problems. *IEEE Trans. Power Syst.* **1999**, *14*, 1114–1120. [CrossRef]
18. Reddy, S.S.; Bijwe, P.R. Efficiency Improvements in Meta-Heuristic Algorithms to Solve the Optimal Power Flow Problem. *Int. J. Emerg. Electr. Power Syst.* **2016**, *17*, 631–647. [CrossRef]
19. Chaib, A.E.; Bouchekara, H.R.E.H.; Mehasni, R.; Abido, M.A. Optimal Power Flow with Emission and Non-Smooth Cost Functions Using Backtracking Search Optimization Algorithm. *Int. J. Electr. Power Energy Syst.* **2016**, *81*, 64–77. [CrossRef]
20. Bouchekara, H.R.E.H.; Chaib, A.E.; Abido, M.A.; El-Sehiemy, R.A. Optimal Power Flow Using an Improved Colliding Bodies Optimization Algorithm. *Appl. Soft Comput. J.* **2016**, *42*, 119–131. [CrossRef]
21. Kumar, A.R.; Premalatha, L. Optimal Power Flow for a Deregulated Power System Using Adaptive Real Coded Biogeography-Based Optimization. *Int. J. Electr. Power Energy Syst.* **2015**, *73*, 393–399. [CrossRef]
22. Basu, M. Modified Particle Swarm Optimization for Nonconvex Economic Dispatch Problems. *Int. J. Electr. Power Energy Syst.* **2015**, *69*, 304–312. [CrossRef]
23. Singh, R.P.; Mukherjee, V.; Ghoshal, S.P. Particle Swarm Optimization with an Aging Leader and Challengers Algorithm for the Solution of Optimal Power Flow Problem. *Appl. Soft Comput. J.* **2016**, *40*, 161–177. [CrossRef]
24. El-Fergany, A.A.; Hasanien, H.M. Single and Multi-Objective Optimal Power Flow Using Grey Wolf Optimizer and Differential Evolution Algorithms. *Electr. Power Compon. Syst.* **2015**, *43*, 1548–1559. [CrossRef]
25. Bouchekara, H.R.E.H.; Chaib, A.E.; Abido, M.A. Optimal Power Flow Using GA with a New Multi-Parent Crossover Considering: Prohibited Zones, Valve-Point Effect, Multi-Fuels and Emission. *Electr. Eng.* **2018**, *100*, 151–165. [CrossRef]
26. El-Hana Bouchekara, H.R.; Abido, M.A.; Chaib, A.E. Optimal Power Flow Using an Improved Electromagnetism-like Mechanism Method. *Electr. Power Compon. Syst.* **2016**, *44*, 434–449. [CrossRef]
27. Ghasemi, M.; Ghavidel, S.; Gitizadeh, M.; Akbari, E. An Improved Teaching-Learning-Based Optimization Algorithm Using Lévy Mutation Strategy for Non-Smooth Optimal Power Flow. *Int. J. Electr. Power Energy Syst.* **2015**, *65*, 375–384. [CrossRef]
28. Ziane, I.; Benhamida, F.; Graa, A. Simulated Annealing Algorithm for Combined Economic and Emission Power Dispatch Using Max/Max Price Penalty Factor. *Neural Comput. Appl.* **2017**, *28*, 197–205. [CrossRef]
29. Dabba, A.; Tari, A.; Meftali, S. Hybridization of Moth Flame Optimization Algorithm and Quantum Computing for Gene Selection in Microarray Data. *J. Ambient Intell. Humaniz. Comput.* **2020**, *12*, 2731–2750. [CrossRef]
30. El-Ela, A.A.A.; El-Sehiemy, R.A.; Shaheen, A.M.; Ellien, A.R. Optimal Allocation of Distributed Generation Units Correlated with Fault Current Limiter Sites in Distribution Systems. *IEEE Syst. J.* **2020**, *15*, 2148–2155. [CrossRef]
31. Bentouati, B.; Javaid, M.S.; Bouchekara, H.R.E.H.; El-Fergany, A.A. Optimizing Performance Attributes of Electric Power Systems Using Chaotic Salp Swarm Optimizer. *Int. J. Manag. Sci. Eng. Manag.* **2020**, *15*, 165–175. [CrossRef]
32. Khalilpourazari, S.; Khalilpourazary, S. An Efficient Hybrid Algorithm Based on Water Cycle and Moth-Flame Optimization Algorithms for Solving Numerical and Constrained Engineering Optimization Problems. *Soft Comput.* **2019**, *23*, 1699–1722. [CrossRef]
33. Pan, J.S.; Shan, J.; Chu, S.C.; Jiang, S.J.; Zheng, S.G.; Liao, L. A Multigroup Marine Predator Algorithm and Its Application for the Power System Economic Load Dispatch. *Energy Sci. Eng.* **2021**. [CrossRef]
34. Bai, Y.; Wu, X.; Xia, A. An Enhanced Multi-Objective Differential Evolution Algorithm for Dynamic Environmental Economic Dispatch of Power System with Wind Power. *Energy Sci. Eng.* **2021**, *9*, 316–329. [CrossRef]
35. Bentouati, B.; Khelifi, A.; Shaheen, A.M.; El-Sehiemy, R.A. An Enhanced Moth-Swarm Algorithm for Efficient Energy Management Based Multi Dimensions OPF Problem. *J. Ambient Intell. Humaniz. Comput.* **2020**, *12*, 9499–9519. [CrossRef]
36. Daryani, N.; Hagh, M.T.; Teimourzadeh, S. Adaptive Group Search Optimization Algorithm for Multi-Objective Optimal Power Flow Problem. *Appl. Soft Comput. J.* **2016**, *38*, 1012–1024. [CrossRef]
37. Nguyen, T.T. A High Performance Social Spider Optimization Algorithm for Optimal Power Flow Solution with Single Objective Optimization. *Energy* **2019**, *171*, 218–240. [CrossRef]
38. Elattar, E.E.; ElSayed, S.K. Modified JAYA Algorithm for Optimal Power Flow Incorporating Renewable Energy Sources Considering the Cost, Emission, Power Loss and Voltage Profile Improvement. *Energy* **2019**, *178*, 598–609. [CrossRef]
39. Li, S.; Gong, W.; Wang, L.; Yan, X.; Hu, C. Optimal Power Flow by Means of Improved Adaptive Differential Evolution. *Energy* **2020**, *198*, 117314. [CrossRef]
40. Warid, W.; Hizam, H.; Mariun, N.; Wahab, N.I.A. A Novel Quasi-Oppositional Modified Jaya Algorithm for Multi-Objective Optimal Power Flow Solution. *Appl. Soft Comput.* **2018**, *65*, 360–373. [CrossRef]
41. Zhang, J.; Wang, S.; Tang, Q.; Zhou, Y.; Zeng, T. An Improved NSGA-III Integrating Adaptive Elimination Strategy to Solution of Many-Objective Optimal Power Flow Problems. *Energy* **2019**, *172*, 945–957. [CrossRef]
42. Elattar, E.E.; Shaheen, A.M.; Elsayed, A.M.; El-Sehiemy, R.A. Optimal Power Flow with Emerged Technologies of Voltage Source Converter Stations in Meshed Power Systems. *IEEE Access* **2020**, *8*, 166963–166979. [CrossRef]
43. Abdollahzadeh, B.; Gharehchopogh, F.S.; Mirjalili, S. Artificial Gorilla Troops Optimizer: A New Nature-Inspired Metaheuristic Algorithm for Global Optimization Problems. *Int. J. Intell. Syst.* **2021**, *36*, 5887–5958. [CrossRef]

44. Ginidi, A.; Ghoneim, S.M.; Elsayed, A.; El-Sehiemy, R.; Shaheen, A.; El-Fergany, A. Gorilla Troops Optimizer for Electrically Based Single and Double-Diode Models of Solar Photovoltaic Systems. *Sustainability* **2021**, *13*, 9459. [CrossRef]
45. Zimmerman, R.D. Matpower [Software]. Available online: https://Matpower.Org (accessed on 1 August 2021).
46. Liu, Y.; Gong, D.; Sun, J.; Jin, Y. A Many-Objective Evolutionary Algorithm Using a One-by-One Selection Strategy. *IEEE Trans. Cybern.* **2017**, *47*, 2689–2702. [CrossRef] [PubMed]
47. Askarzadeh, A. A Novel Metaheuristic Method for Solving Constrained Engineering Optimization Problems: Crow Search Algorithm. *Comput. Struct.* **2016**, *169*, 1–12. [CrossRef]
48. Horng, S.C.; Lin, S.S. Bat Algorithm Assisted by Ordinal Optimization for Solving Discrete Probabilistic Bicriteria Optimization Problems. *Math. Comput. Simul.* **2019**, *166*, 346–364. [CrossRef]
49. Shaheen, A.M.; El-Sehiemy, R.A.; Elsayed, A.M.; Elattar, E.E. Multi-Objective Manta Ray Foraging Algorithm for Efficient Operation of Hybrid AC/DC Power Grids with Emission Minimisation. *IET Gener. Transm. Distrib.* **2021**, *15*, 1314–1336. [CrossRef]
50. El-Sehiemy, R.; Elsayed, A.; Shaheen, A.; Elattar, E.; Ginidi, A. Scheduling of Generation Stations, OLTC Substation Transformers and VAR Sources for Sustainable Power System Operation Using SNS Optimizer. *Sustainability* **2021**, *13*, 11947. [CrossRef]
51. Shaheen, A.M.; El-Sehiemy, R.A. Application of Multi-Verse Optimizer for Transmission Network Expansion Planning in Power Systems. In Proceedings of the International Conference on Innovative Trends in Computer Engineering ITCE 2019, Aswan, Egypt, 2–4 February 2019; pp. 371–376. [CrossRef]
52. Taher, M.A.; Kamel, S.; Jurado, F.; Ebeed, M. An Improved Moth-Flame Optimization Algorithm for Solving Optimal Power Flow Problem. *Int. Trans. Electr. Energy Syst.* **2019**, *29*, e2743. [CrossRef]
53. Abdo, M.; Kamel, S.; Ebeed, M.; Yu, J.; Jurado, F. Solving Non-Smooth Optimal Power Flow Problems Using a Developed Grey Wolf Optimizer. *Energies* **2018**, *11*, 1692. [CrossRef]
54. Duman, S. Symbiotic Organisms Search Algorithm for Optimal Power Flow Problem Based on Valve-Point Effect and Prohibited Zones. *Neural Comput. Appl.* **2017**, *28*, 3571–3585. [CrossRef]
55. Ghanizadeh, A.J.; Mokhtari, M.; Abedi, M.; Gharehpetian, G.B. Optimal Power Flow Based on Imperialist Competitive Algorithm. *Int. Rev. Electr. Eng.* **2011**, *6*, 4–12.
56. Alhejji, A.; Hussein, M.E.; Kamel, S.; Alyami, S. Optimal Power Flow Solution with an Embedded Center-Node Unified Power Flow Controller Using an Adaptive Grasshopper Optimization Algorithm. *IEEE Access* **2020**, *8*, 119020–119037. [CrossRef]
57. Bouchekara, H.R.E.H. Optimal Power Flow Using Black-Hole-Based Optimization Approach. *Appl. Soft Comput. J.* **2014**, *24*, 879–888. [CrossRef]
58. Shaheen, A.M.; El-Sehiemy, R.A.; Elattar, E.E.; Abd-Elrazek, A.S. A Modified Crow Search Optimizer for Solving Non-Linear OPF Problem with Emissions. *IEEE Access* **2021**, *9*, 43107–43120. [CrossRef]
59. Mohamed, A.A.A.; Mohamed, Y.S.; El-Gaafary, A.A.M.; Hemeida, A.M. Optimal Power Flow Using Moth Swarm Algorithm. *Electr. Power Syst. Res.* **2017**, *142*, 190–206. [CrossRef]
60. Jeddi, B.; Einaddin, A.H.; Kazemzadeh, R. A Novel Multi-Objective Approach Based on Improved Electromagnetism-like Algorithm to Solve Optimal Power Flow Problem Considering the Detailed Model of Thermal Generators. *Int. Trans. Electr. Energy Syst.* **2017**, *27*, e2293. [CrossRef]
61. Yang, X.S. Bat Algorithm: Literature Review and Applications. *Int. J. Bio-Inspired Comput.* **2013**, *5*, 141–149. [CrossRef]
62. Shaheen, A.M.; El-Sehiemy, R.A.; Ginidi, A.R.; Ghoneim, S.S.M.; Alharthi, M.M. Multi-Objective Jellyfish Search Optimizer for Efficient Power System Operation Based on Multi-Dimensional OPF Framework. *Energy* **2021**, *237*, 121478. [CrossRef]
63. Pulluri, H.; Naresh, R.; Sharma, V. A Solution Network Based on Stud Krill Herd Algorithm for Optimal Power Flow Problems. *Soft Comput.* **2018**, *22*, 159–176. [CrossRef]
64. Shabanpour-Haghighi, A.; Seifi, A.R.; Niknam, T. A Modified Teaching-Learning Based Optimization for Multi-Objective Optimal Power Flow Problem. *Energy Convers. Manag.* **2014**, *77*, 597–607. [CrossRef]
65. Shaheen, A.M.; Elsayed, A.M.; El-Sehiemy, R.A.; Ghoneim, S.S.M.; Alharthi, M.M.; Ginidi, A.R. Multi-Dimensional Energy Management Based on an Optimal Power Flow Model Using an Improved Quasi-Reflection Jellyfish Optimization Algorithm. *Eng. Optim.* **2022**, 1–23. [CrossRef]